Discovery of Small Molecules That Induce Lysosomal Cell Death in Cancer Cell Lines Using an Image-Based Screening Platform

Romina J. Pagliero,[1,] Diego S. D'Astolfo,[1,2] Daphne Lelieveld,[1] Riyona D. Pratiwi,[1] Sonja Aits,[3] Marja Jaattela,[3] Nathaniel I. Martin,[4] Judith Klumperman,[1] and David A. Egan[1]*

[1]Department of Cell Biology, University Medical Center Utrecht (UMCU), Utrecht, the Netherlands.
[2]KNAW-Hubrecht Institute, Utrecht, the Netherlands.
[3]Cell Death and Metabolism Unit, Center for Autophagy, Recycling and Disease, Danish Cancer Society Research Center, Copenhagen, Denmark.
[4]Department of Chemical Biology and Drug Discovery, Utrecht Institute for Pharmaceutical Sciences (UIPS), Utrecht University, Utrecht, the Netherlands.
**Present address: Genmab B.V., Utrecht, the Netherlands.*

ABSTRACT

The lysosomal cell death (LCD) pathway is a caspase 3-independent cell death pathway that has been suggested as a possible target for cancer therapy, making the development of sensitive and specific high-throughput (HT) assays to identify LCD inducers highly desirable. In this study, we report a two-step HT screening platform to reliably identify such molecules. First, using a robust HT primary screen based on propidium iodide uptake, we identified compounds that kill through nonapoptotic pathways. A phenotypic image-based assay using a galectin-3 (Gal-3) reporter was then used to further classify hits based on lysosomal permeabilization, a hallmark of LCD. The identification of permeabilized lysosomes in our image-based assay is not affected by changes in the lysosomal pH, thus resolving an important limitation in currently used methods. We have validated our platform in a screen by identifying 24 LCD inducers, some previously known to induce LCD. Although most LCD inducers were cationic amphiphilic drugs (CADs), we have also identified a non-CAD LCD inducer, which is of great interest in the field. Our data also gave new insights into the biology of LCD, suggesting that lysosomal accumulation and acid sphingomyelinase inhibition are not sufficient or necessary for the induction of LCD. Overall, our results demonstrate a robust HT platform to identify novel LCD inducers that will also be very useful for gaining deeper insights into the molecular mechanism of LCD induction.

Keywords: lysosomal cell dead, galectin-3 reporter, LMP phenotypic assay, high throughput screening

INTRODUCTION

Apoptosis is a universal, caspase-dependent cell death pathway, which is the target of many cancer therapies. However, tumor cells often harbor genetic mutations that make them resistant to apoptotic cell death. Many changes conferring resistance to apoptosis have been observed, such as mutations in the gene encoding p53 (*TP53*), which are found in 50% of solid tumors.[1,2] In breast and prostate cancers, increased expression of the antiapoptotic B-Cell lymphoma 2 protein (Bcl2) blocks the apoptotic pathway.[3] Therefore, the induction of cell death in cancer cells by pathways that are caspase-3, p53, or Bcl2 independent is very interesting for the development of novel anticancer treatments. One such alternative cell death pathway is lysosomal cell death (LCD) that has been proposed in recent years as a possible target for cancer therapy.[4]

Lysosomes are digestive organelles that are essential for cell homeostasis.[5,6] They act as a cell recycling center and receive cargo mainly through autophagy and endocytosis. Apart from their function in general protein and organelle turnover, lysosomes are also involved in processes such as the control of cell cycle progression, antigen presentation, epidermal homeostasis, and hair follicle morphogenesis.[7] Remarkably, lysosomes have also been shown to be important players in triggering programmed cell death (PCD).

Lysosomal membrane permeabilization (LMP) and the subsequent release of lysosomal hydrolases into the cytosol are the main hallmark of LCD (also called LMP-induced apoptosis-like PCD).[8–11] Cathepsin B, L, and D, abundant in lysosomes, are among the best defined effector molecules for LCD.[12–14] Nevertheless, their inhibition often confers only partial protection against LMP-induced cell death, suggesting the possible involvement of other lysosomal enzymes. Although the precise mechanisms of LMP and the role of the released lysosomal enzymes in cell death are still largely unknown, it is clear that LMP can be triggered by a wide variety of stimuli such as death receptor activation, microtubule-stabilizing agents, oxidative stress, growth factor deprivation, sphingosine, and other compounds.[14,15]

Interestingly, upon transformation, many tumor cells are subject to changes in their lysosomal system that selectively

increase their vulnerability to LMP.[16,17] For example, the expression levels of cathepsin D, cathepsin B, and other cysteine cathepsins are significantly upregulated in many human cancers.[16,17] In addition, the number of lysosomes can be increased in cancer cells.[18] Importantly, higher expression of cathepsin B leads to increased degradation of lysosomal-associated membrane protein (LAMP)-1 and -2, which in turn increases the susceptibility to LMP.[19] Thus, the changes that occur in the lysosomal system of cancer cells sensitize them to LCD.[12,20]

Because compounds that induce alternative cell death pathways may be able to eradicate tumors that are resistant to classical therapies, we decided to develop a high-throughput (HT) screening platform to identify such compounds. Phenotypic image-based assays are highly informative for the elucidation of the mechanism of action of bioactive compounds,[21,22] so we developed such an assay to identify compounds that can trigger LCD by measuring LMP.

Until now, the development of high-throughput screening (HTS) strategies for the discovery of LCD-triggering compounds has been hampered by the lack of an appropriate method to detect LMP. Most reagents used to fluorescently label lysosomes are fluorophores linked to a weak base. Under physiological conditions, these lysosomal dyes accumulate inside lysosomes due to the pH gradient and are trapped upon protonation, becoming fluorescent (*e.g.*, LysoTracker dyes).[23] Consequently, basic drugs, such as cationic amphiphilic drugs (CADs), which accumulate in lysosomes and affect their pH, can reduce the dye fluorescence even when not causing LMP.[8,24,25] Other methods used to measure LMP are based on cytosolic extraction and measurement of enzymatic activity within the cytosol.[26] These assays require numerous steps and delicate manipulation of samples for the efficient and reliable extraction of the cytosol, making them very error prone and difficult to adapt to an HTS setting.

An alternative method measures LMP by galectin translocation. Galectins are small soluble proteins normally found in the cytosol, which can bind beta-galactoside sugar-containing carbohydrates. These carbohydrates are normally present only on the exterior of the plasma membrane; and on the interior of intracellular endocytic vesicles, where they become accessible to cytosolic galectins after vesicle permeabilization. Galectin-3 (Gal-3) and -8 have previously been used to measure vacuole lysis promoted by invasive pathogens.[27–30] We have also described the use of Gal-3 to visualize and quantify macropinosome leakage during induced transduction by osmocytosis and propanebetaine.[31] Recently, we have validated the detection of galectin puncta as a reporter to measure LMP.[32] Gal-1, -3, -8, and -9 translocate rapidly from their diffuse cytosolic localization to permeable lysosomes during LCD, thereby forming cytoplasmic puncta. The formation of these puncta occurs regardless of the stimuli used to induce LMP and is maintained for several hours. These characteristics make galectins an excellent reporter system for the development of a live-cell image-based assay for the detection of LMP and identification of LCD triggering compounds in a HT setting.

In this study, we describe the development of a two-step screening platform that allows the rapid identification of compounds that induce alternative cell death pathways with particular emphasis on LMP as a mechanism of action. The primary screen is a robust, highly scalable fluorescence-based HT assay that uses a genetically modified cell line to discard the compounds that kill only through classical apoptosis, thus identifying those that induce caspase-3 and Bcl2-independent alternative cell death pathways. The secondary screen uses an image-based assay with a Gal-3 reporter cell line, which allows for the characterization of the hits as LCD inducers.

Using our platform, we were able to correctly identify several previously known LCD inducers, validating our strategy, but the screen also revealed LCD inducers that had not been previously identified. Our phenotypic screening platform is robust, rapid, and sensitive and it constitutes a versatile system that can be used to quickly identify novel LCD inducers. We discuss the perspectives of this screening platform that can also be used to further investigate the poorly understood LCD pathway.

MATERIALS AND METHODS

Chemicals

Propidium iodide (PI, P4170) and Hoechst 33342 (14533) were purchased from Sigma-Aldrich (P4170). Calcein-AM (C3099) and LysoTracker® Red DND-99 (L7528) were from Thermo-Fisher Scientific. The pan-caspase inhibitor Z-VAD-FMK was from Bachem (N1510.0005). Necrostatin-1 (N9037) and staurosporine (S5921) were from Sigma-Aldrich. Prestwick Chemical library used for the screening was acquired from Prestwick Chemical, France. For the confirmation screening, selected compounds were purchased as single 10 mg vials from Prestwick Chemicals (France), unless otherwise indicated (See *Supplementary Experimental Procedures*; Supplementary Data are available online at www.liebertpub.com/adt). All other chemicals were obtained from Sigma-Aldrich, unless otherwise indicated.

Synthesis of Siramesine

Siramesine was synthesized using a modification of the protocol of Perregaard *et al.*[33] *Supplementary Figure S1* summarizes the synthetic strategy of siramesine. In brief, commercially available 4-(1H-indol-3-yl)-butanoic acid (**1**) was converted to 4-(1H-indol-3-yl)-butanol (**2**) by first producing the methyl ester (**1a**) followed by its reduction with $LiAH_4$ to generate the mentioned alcohol. 4-(1H-indol-3-yl)-butanol was arylated using the

Ullmann procedure to obtain 4-[1-(4-fluorophenyl)-1H-indol-3-yl)-butanol (**3**). The spiro-[isobenzofuran-1(3H),4′-piperidine] (**4**) was synthesized as previously described by Sommer *et al.*[34] Finally, siramesine (**5**) was obtained by amine alkylation of this spiro-piperidine heterocycle (**4**) with the methanesulfonate ester of 3 (**3a**). Detailed information of the synthetic route and the materials used during the synthesis of siramesine is included in *Supplementary Experimental Procedures.*

Cell Culture

MCF7-Bcl2 cells and MCF7-Casp3 cells have been described elsewhere.[20,32,35] U2OS-mCherry-Gal3 cells were kindly provided by Dr. Harald Wodrich (Laboratoire de Microbiologie Fondamentale et Pathogénicité, Bordeaux, France).[36] All MCF7 cells were maintained in basic culture media of high-glucose Dulbecco's modified Eagle's medium (DMEM) supplemented with 10% fetal calf serum, 100 U/mL of penicillin, and 100 μg/mL of streptomycin. Selection antibiotics were as follows: Hygromycin B (150 μg/mL) for MCF7-Bcl2 cells, G418 (200 μg/mL) for MCF7-Casp3 cells, and puromycin (2 μg/mL) for MCF7-mAG-Gal3 cells.

HT PI Cytotoxicity Assay

MCF7 cells were seeded in black clear-bottom 96-well plates at 30,000 cells/well (93,750 cell/cm^2) in 80 μL/well of basic culture medium and they were allowed to attach overnight.

Table 1. High-Throughput Propidium Iodide Cytotoxicity Assay

Step	Parameter	Value	Description
1	Plate cells	80 μL	30,000 MCF7-Bcl2 cell/well (93,750 cells/cm^2)
2	Dilution of library	60 μL	Serial dilution in DMSO. All concentrations are 200× from final concentration on cells.
3	Compound treatment	20 μL	Final concentration from 3 to 60 μM
4	Control treatment	20 μL	Siramesine (60 μM), Staurosporine (5 μM), DMSO (0.5%, vehicle)
5	Incubation time	24 h	37°C, 5% CO_2
6	Read out; reagent I	50 μL	Propidium Iodide, 30 μM
7	Incubation time	30 min	37°C, 5% CO_2
8	Read out I	ex/em 544/624 nm	Fluorescence
9	Read out; reagent II	50 μL	Triton X-100, 3.2% in PBS
10	Read out II	ex/em 544/624 nm	Fluorescence
11	Incubation time	15–30 min	Room temperature
12	Calculations	–	Calculate % dead cells, calculate LC_{50}

Step Notes

1. Use black-walled clear-bottom 96-well plates. Dispense cells with multichannel or Multidrop dispenser. Incubate 24 h for attachment before adding compounds.
2. *Optional step if LC_{50} is to be measured.* Compounds are store in 96-well plates at a concentration of 20 mM. Serial dilution in 384 wells polypropylene V-bottom storage plates. Dilution per quadrant (Q1 to Q4). Two-stage serial dilutions. Plate 1: From 12 mM, serial dilution factor of 2. Plate 2: From 9.6 mM, serial dilution factor of 2.
3. The library is located in columns 2–11. From DMSO 200× solutions (step 2), dilute the library 40 times in media using 384-well polystyrene V-bottom plates. Add 20 μL of this solution to 96-well plates containing cells. Dispense compounds per quadrant, 96-tip. Each concentration (quadrant) in different cell plates. Triplicate plates per concentration. Tip wash sequence between plates: DMSO, MeOH, water, MeOH, Air Dry.
4. Controls are located in columns 1 and 12. Same details as step 3, but dispense controls in plates with 8-tip.
6. Dilute PI Stock solution (1.5 mM) to 30 μM in PBS. Dispense reagents in all wells, 96-tip. Final concentration is 10 μM.
8. Read in fluorescence plate reader, SpectraMaxPlus (Molecular Devices). Read time is 1 min per plate.
9. Dispense reagent in all wells, 96-tip. Final concentration is 0.8%.
11. Incubation should not exceed 30 min.
12. $$\%\ \text{Dead Cells} = \frac{[\text{Read out I (sample)} - \text{Read out I (DMSO)}]}{[\text{Read out II (sample)} - \text{Read out II (DMSO)}]} \times 100$$

Bcl2, B-cell lymphoma 2 protein; DMSO, dimethyl sulfoxide; LC_{50}, concentration that is lethal to 50% of cells; MeOH, methanol; PBS, phosphate-buffered saline; PI, propidium iodide.

Stock solutions (200 times more concentrated) were prepared for all compounds in dimethyl sulfoxide (DMSO). For LC_{50} determination, compound serial dilutions were prepared as outlined in *Table 1*. Using an automatic liquid handler (Sciclone G3 Automated Liquid Handling Workstation; PerkinElmer), stock solutions were diluted 40 times in culture medium and then 20 μL of each solution was added to the cells. DMSO 0.5% was used as vehicle control. In the final plate layout, test compounds were added to the well in columns 2–11. Siramesine, staurosporine, and DMSO 0.5% were included in all plates, in columns 1 and 12, in five replicates each. The cells were treated for 24 h at 37°C, 5% CO_2. Fifty microliters of staining solution (30 μM PI in phosphate buffered saline [PBS]) was added to each well. The cells were further incubated for 30 min at 37°C, and fluorescence was measured with a SpectraMAXPlus (Molecular Devices, Sunnyvale, CA) microplate reader at excitation/emission wavelengths of 544/624 nm. Immediately after, 50 μL of a solution of 3.2% Triton X-100 was added to each well, and cells were incubated 15–30 min at room temperature before reading the fluorescence again. To eliminate autofluorescent compounds, plates were read once at 544/624 nm before the addition of PI. The assay Z′-factor and signal to noise (S/N) were calculated in a pilot screen using 48 wells with siramesine (30 μM) and 48 wells with DMSO 0.5% randomly distributed within the plate. $Z' = 1 - 3(\sigma p + \sigma n)/|\mu p - \mu n|$, where μp and σp are the mean and standard deviation (SD), respectively, of the positive control (siramesine), and μn and σn are the mean and SD, respectively, of the negative control (DMSO).[37] The calculated assay Z′-factors for five independent plates were between 0.8 and 0.95 with a mean of 0.86 indicating a robust and reliable assay.

Cytotoxicity data analysis/LC_{50}. The percentage of dead cells was calculated by dividing the "dead cells fluorescence" (first reading) by the "total cells fluorescence" (second reading) and multiplying by 100. The mean of samples treated with DMSO 0.5% was used as Background subtraction. The Z′-factor was calculated for each plate based on the controls and was >0.5 in all cases.[37] Hit threshold was set as three times the SD of the mean of the negative control (DMSO) as previously described.[37] For LC_{50} calculation, the percentage of dead cells at each concentration (mean, $n = 3$) was used to calculate the LC_{50} from a best-fit curve with a nonlinear regression model using GraphPad Prism 5.0 software. All values are indicated as $LC_{50} \pm$

Table 2. Image-Based Lysosomal Membrane Permeabilization Screening Assay

Step	Parameter	Value	Description
1	Plate cells	100 μL	12,500 U2OS-mCherryGal3 cell/well (39,000 cells/cm^2).
2	Incubation time	24 h	37°C, 5% CO_2
3	Compound treatment	0.3 μL	3–30 μM (final concentration). Lineal serial dilution 1.3×
4	Controls treatment	0.3 μL	Siramesine (positive, 23 μM), staurosporine (negative, 5 μM), DMSO (vehicle, 0.3%)
5	Incubation time	6 h	37°C, 5% CO_2
6	Staining solution	10 μL	27.5 μM Hoechst and 11 μM Calcein-AM in PBS
7	Incubation time	30 min	37°C, 5% CO_2
8	Read out	20× objective	10 fields with at least 500 cells/well. Autofocus in Channel 1 (Hoechst, nuclei)
9	Image quantification		Thermo Scientific™ HCS Studio Cell Analysis Software, Spot Detector Bioapplication

Step Notes

1. Use black-walled, clear-bottom 96-well plates. Dispense cells with multichannel or Multidrop dispenser. Incubate 24 h for attachment before adding compounds.
3. The library is located in columns 2–11. Concentration curves run from Columns 2 to 11. Dispense compounds from Stocks 20 mM in DMSO with a TECAN digital dispenser. DMSO was normalized to 0.3%. Duplicate concentration curves are located in duplicate plates.
4. Controls are located in columns 1 and 12. Addition as in step 3.
6. Ninety-six-tip dispense reagent to all wells. Staining solution must be prepared just before use.
8. Channels: Channel 1, XF93-Hoechst, Channel 2, XF93-TRITC, and Channel 3. XF93-FITC. Exposures in all channels were set as fixed exposure, based on the vehicle (negative control) and the siramesine-treated cells (positive control).
9. Object identification in Channel 1 (Hoechst). Border touching objects were rejected. Spots were quantified in Channel 2 (mCherry-Galectin-3) according to parameters in *Table 3*.

HCS, high content screening.

95% confidence interval (95% CI). To evaluate if two calculated LC_{50}s were significantly different, we perform an "Extra sum-of-squares F-Test" (GraphPad Prism 5.0 software) comparing the best-fitted models and determine the *P* value to evaluate the null hypothesis "LC_{50}s are the same in both data sets." When the *P* value was >0.05, the LC_{50}s were accepted as being the same.

Image-Based Assay to Measure LMP

U2OS-mCherry-Gal3 cells were seeded in black clear-bottom 96-well plates at 12,500 cells/well (39,000 cell/cm^2) as described in *Table 2*, and they were allowed to attach overnight at 37°C, 5% CO_2. Because siramesine and possibly all LCD inducers are sensitive to the density of cells at the time of treatment, the number of seeded cells is an essential parameter.[20] For the LMP assay, the density of U2OS cells was adjusted from that used in the PI-Cytotoxicity assay, considering the difference in growth rate between U2OS versus MCF7 cells, to have the same density at the moment of compound treatment. Compounds were automatically added to the cells from a 20 mM DMSO stock, in linear 1.3× serial dilutions using a TECAN HPD300e Digital Dispenser (Hewlett-Packard) to establish a dose–response curve for each compound. DMSO percentage was normalized to 0.3% on each well; wells with just 0.3% DMSO served as a vehicle control. Duplicate samples for each concentration were analyzed on separate plates.

The cells were treated with the 50 selected compounds, siramesine (23 μM), staurosporine (5 μM), and vehicle. In the final plate layout, the test compounds were distributed in columns 2–11, with dose–response curves running from column 1 to 11. Siramesine, staurosporine, and the vehicle were included in all plates, randomly distributed in columns 1 and 12, in five replicates each. In addition, siramesine and staurosporine were included within the compounds and were also tested in dose–response. After 6 h of treatment at 37°C, 5% CO_2, we added 10 μL of staining solution (27.5 μM Hoechst and 11 μM Calcein-AM) to each well. The cells were further incubated for 30 min at 37°C, 5% CO_2. The plates were sealed and imaged with a Thermo Fisher CellInsight™ CX5 high-content screening (HCS) Reader using a 20× objective.

Image acquisition was set to a maximum of 10 fields per well with a minimum of 500 cells/well. Image analysis was performed using Thermo Scientific™ HCS Studio Cell Analysis Software with the Spot Detector Bioapplication as shown in *Table 3*. First nuclei were identified in channel 1 (Hoechst) and were gated based primarily on their intensity (>43). Border touching objects were rejected. Clumped nuclei were segmented based on the differences in intensities (>134) and only nuclei that had an Object.Area.Ch1 within 703–3,515 were considered as viable nuclei. Nuclei were also selected based on their shape, Object.Shape.P2A (1.0–2.54), and Object.Shape.LWR (1.0–5.0). Viability was further analyzed using Calcein-AM in channel 3. A cell mask was defined around each nucleus (MaskRingWidthCh3 = 29). Only cells with an Object.Total.Intensity.Ch3 > 50 were considered as viable cells. Gal-3 relocation to lysosomes was quantified as punctate signal

Table 3. CellInsight CX5 Settings for Lysosomal Membrane Permeabilization Screening Assay

Channel	Description	Value
Channel 1: Hoechst		
Dye/channel	Hoechst 33342	Excited at 386
Exposure	Fix	0.01
Thresholding	Fixed intensity	43
Segmentation	Intensity	134
Smooth factor		3
Background correction		50
Object.Area.Ch1		703–3,515
Object.Shape.P2A.Ch2		1.0–2.54
Object.Shape.LWR.Ch2		1.0–5.0
Border touching objects		Rejected
Channel 2: mCherry-Gal3		
Dye/channel	mCherry-Gal3 (expressed)	Excited at 549
Exposure	Fix	0.19
Thresholding	Fixed intensity	200
Segmentation	Intensity	1
Background correction		20
Circle.Modifier.Ch2		21 pixels
Spot.Detect.RadiusCh2		2
Object.Area.Ch2		3.39–102.69
Object.Shape.P2A.Ch2		0–6.17
Object.Total.Intensity.Ch2		81/∞
Channel 3: Calcein-AM		
Dye/channel	Calcein-AM	Excited at 488
Exposure	Fix	0.001
Thresholding	Fixed intensity	130
Background correction		80
Mask.Ring.With.Ch3		29 pixels
Object.Total.Intensity.Ch3		50

(Spots) in channel 2. Spots were gated based on their intensity (>200) and segmented based on the differences in intensities (>1). Spots were quantified within a circular area defined in Ch2 around each object identified in Ch1 (Circle.Modifier.Ch2 = 21 pixels). The spots were discriminated based on their shape, area, and total intensity (*Table 3*). Excessively large or excessively small areas of high intensity were not considered. The limit in the maximum Object.Shape.P2A.Ch2 (6.17) and a Spot.Detect.RadiusCh2 (2) were essential to guarantee that apoptotic blebbing observed in some samples and staurosporine were not recognized as "spots." Although spots were well segmented, they were usually tightly clumped together after treatment. Therefore, the Mean_SpotNumberPerCell resulted in an underestimation of the Gal-3 puncta. The Mean_SpotAreaPerObject was then selected to determine whether a compound induced LMP.

The assay Z′-factor and S/N were calculated in a pilot screen of three plates, each consisting of 32 wells with siramesine (23 μM), 32 wells with staurosporine (5 μM), and 32 wells with DMSO (0.3%) randomly distributed within the plate. For each plate, the Z′-factor was calculated from the positive control (siramesine) and the negative control (staurosporine) and was >0.4 in all cases with a mean of 0.62, indicating the assay is robust and reliable for HTS. During the screen, the controls were included in all plates at the same concentration used during the pilot screen, in five replicates each, and were used to calculate the Z′-factor for each individual plate. The Z′-factor was between 0.39 and 0.7 for all screened plates.[37] The signal to background (S/B) and S/N were calculated across all screen plates and were 10 and 18, respectively.

From the dose–response curves, we selected an optimal concentration as one where mCherry-Gal3 spots were abundant but cells showed low cytotoxicity (less than 10% of dead cells by Calcein-AM staining and roundness). The selected concentration was further used to determinate if the increase in mCherry-Gal3 spot area per cell was significant by comparison with the negative control (staurosporine). The *P* values for samples versus staurosporine were calculated with GraphPad Prism 5 (San Diego, CA) using a *t*-test with two-tailed distribution and considering equal variance of the samples.

Reporter Plasmids and Generation of Reporter Cell Line

The generation of the mAG-Gal3 reporter plasmid (Plasmid #62734; Adgene) was described elsewhere.[9] In brief, Phage2 lentiviral plasmid containing EF1a-RFP-ires-PuroR was digested with Nco1 and BamH1 to remove the RFP sequence. The linearized vector was gel purified, and reporter DNA sequences were PCR amplified and inserted into the linear vector by using the In-Fusion Kit (638909; Clontech). The Gal-3 reporter vectors contain the elements EF1a-mAG-Gal3-ires-PuroR. MCF7-mAG-Gal3 reporter cells lines were made by transduction of cells with lentiviral particles containing the reporter sequences. After 2 days of lentiviral transduction, cells were selected and maintained in basic culture media supplemented with 1 μg/mL of puromycin.

Immunofluorescence Staining and Confocal Microscopy

Cells were grown on glass cover slips in 24-well plates and treated with the compounds as indicated. Cells were fixed for 15 min in 4% paraformaldehyde, permeabilized with ice cold methanol for 5 min, and quenched with 50 mM of NH_4Cl/PBS for 10 min. We then applied blocking buffer (PBS 1% bovine

Fig. 1. Development of a cell-based HT screening assay to identify compounds that induce alternative cell death pathways. **(A)** Workflow of the *PI Cytotoxicity Assay*. Cells were treated for 24 h with compounds before labeling with PI and measuring fluorescence (dead cells). Then, cells were treated with 0.8% of Triton X-100 to permeabilize all cells, and fluorescence was measured again (total cells). The percentage of dead cells per well was calculated with the formula: dead cells/total cells ×100. **(B)** Graphic representation of raw fluorescence values for the first (dead cells, *blue square*) and second (total cells, *red triangle*) reading. MCF7 cells were exposed 24 h to siramesine at 12 different concentrations from 2 to 50 μM. **(C)** Cytotoxicity dose–response curve of siramesine in MCF7 cells derived from values in **(B)**. An $LC_{50} \pm 95\%$ CI of 33.2 ± 2.8 μM ($R^2 = 0.906$) was determined from the mean and SD ($n = 3$) of the calculated % dead cells (*green circle*) using a best-fit curve with a nonlinear regression model (*green line*) with GraphPad Prism 5.0. Data are representative of five individual experiments. **(D)** Cytotoxicity dose–response of siramesine on MCF7-wt (*green square*), MCF7-Bcl2 (*blue diamond*), and MCF7-Casp3 (*red circle*). Cells were treated for 24 h at eight different concentrations ranging from 1 to 60 μM. The percentage of dead cells is plotted as mean ± SD ($n = 3$) and is used to calculate the LC_{50} from a best-fit curve with a nonlinear regression model using GraphPad Prism 5.0. For siramesine: $LC_{50\ (MCF7\text{-}wt)} = 36.3 \pm 3.0$ μM, $LC_{50\ (MCF7\text{-}Bcl2)} = 34.9 \pm 4.6$ μM, $LC_{50\ (MCF7\text{-}Casp3)} = 33.8 \pm 2.5$ μM; F-test (GraphPad Prism 5.0) showed no difference between all three LC_{50} values ($P = 0.48$). **(E)** Cytotoxicity dose–response of staurosporine measure as in D. $LC_{50\ (MCF7\text{-}Casp3)} = 5.4 \pm 2.0$ μM calculated from a best-fit curve with a nonlinear regression model using GraphPad Prism 5.0 software. **(F)** The *PI Cytotoxicity Assay* described in **(A)** was automated and used to screen 1,280 compounds from the Prestwick library. MCF7-Bcl2 cells were treated for 24 h at 50 μM. The values are percentages of dead cells for the library compounds (*blue circle*), siramesine (LCD inducers, *red circle*), and staurosporine (apoptosis inducer, *green circle*). Hit threshold was set to 10% of dead cells corresponding to 3SD of DMSO control (*red line*). Prestwick library autofluorescent compounds (*white circle*) were discarded. A list of the calculated % dead cells for all selected compounds can be found in *Table 4*. CI (95%), 95% confidence interval; Bcl2, B-cell lymphoma 2 protein; Casp3, caspase 3; DMSO, dimethyl sulfoxide; HT, high throughput; LC_{50}, concentration that is lethal to 50% of cells; PI, propidium iodide; SD, standard deviation.

serum albumin) for 1 h following incubation with a primary anti-cathepsin D antibody (1:150, Cat#AF1014; R&D Systems). After washing three times with PBS, we incubated cells 1 h in the dark with secondary goat anti-rabbit Alexa Fluor 488 antibody (1:400, A-11008; Thermo Fisher Scientific). Cells were stained with ProLong Gold Antifade mounting media with DAPI (P36935; Thermo Fisher Scientific) and subjected to imaging.

For live-cell confocal images, cells were seeded on a four-well 35-cm glass bottom dish (627870; Greiner Bio One) to a density of 70,000 cells/well and grown overnight. The following day, cells were treated with compounds or DMSO as indicated and labeled with 6 μM Hoechst 33342 for nuclear visualization and/or 25 nM LysoTracker-Red. We incubated cells for 30 min and imaged them on a Zeiss LSM 520 confocal microscope using an Apochromat 63×/1.40 Oil DIC M27 objective and Zen

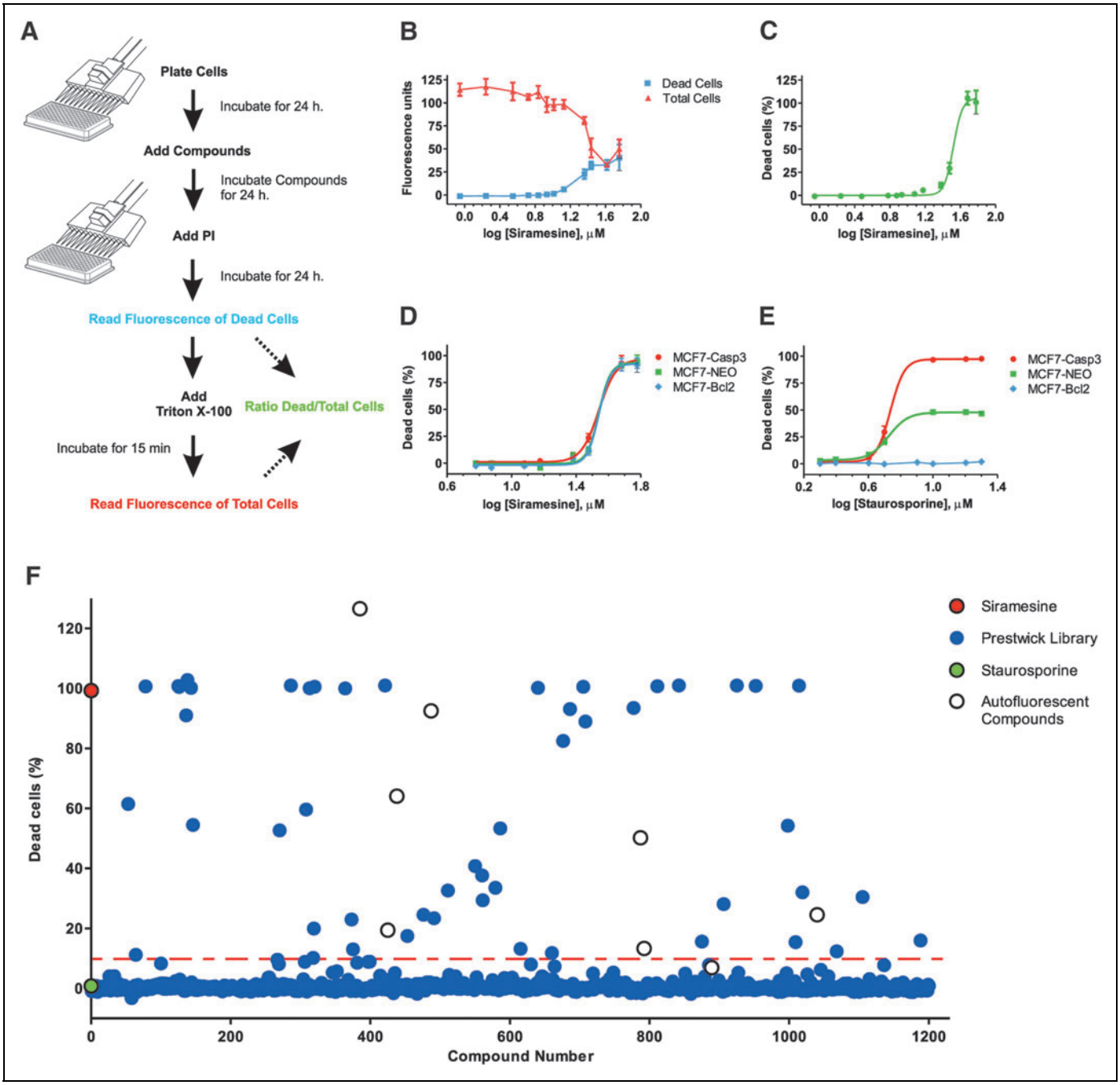

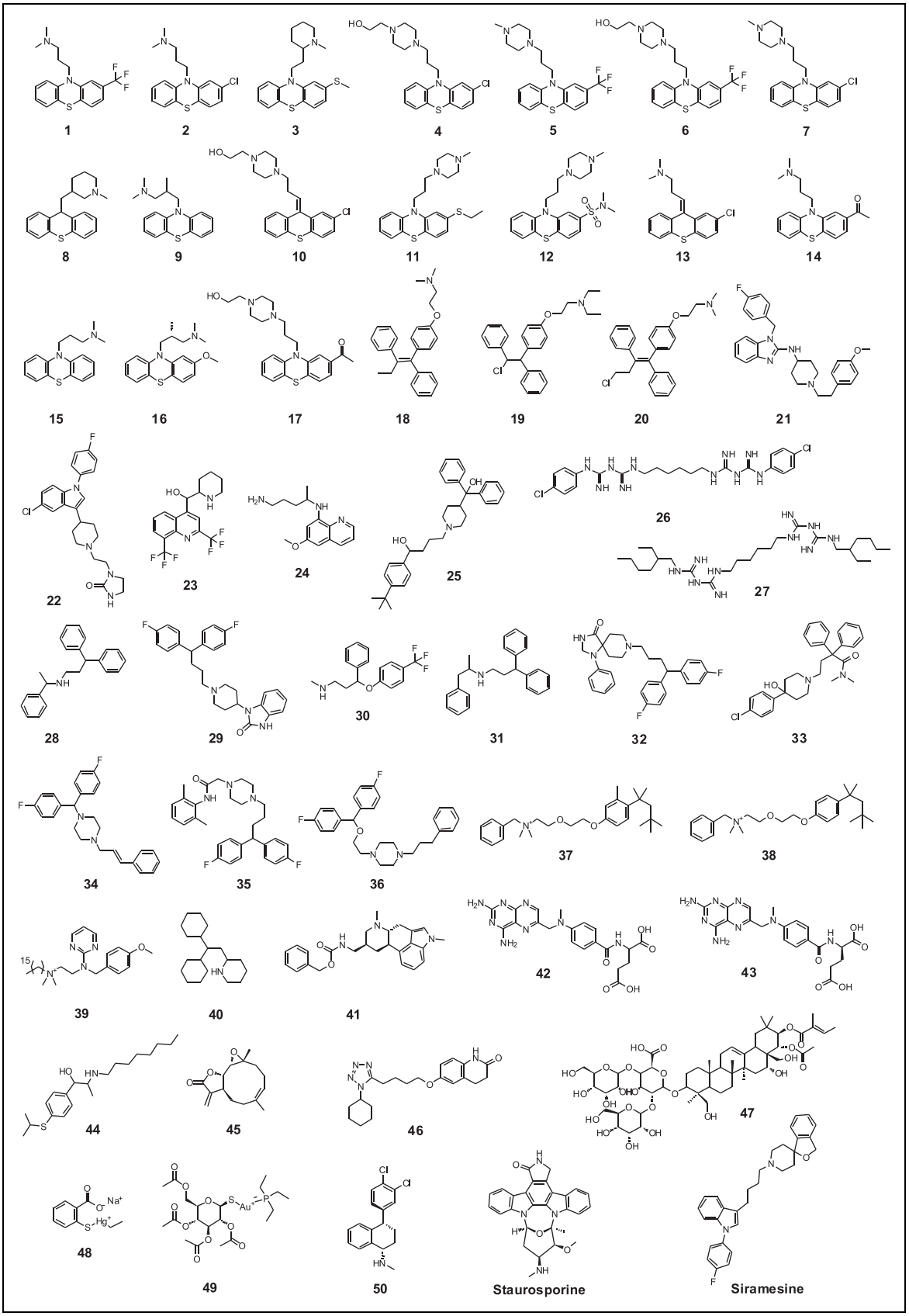

Fig. 2. Chemical structures for compounds selected during the primary screening.

2010 software (all equipment and software from Carl Zeiss, Jena, Germany). Pinhole size was set such that the section thickness was equal for all channels.

RESULTS

Development of a Cell-Based HTS Assay to Identify Small Molecules That Induce Caspase-3-Independent Cell Death

We designed a primary screen to select compounds that can induce alternative cell death pathways while discarding those that can only kill through apoptosis. The screen was based on a simple, homogeneous HT assay that measures cell death using PI staining in apoptosis-resistant cells.

PI is an inexpensive fluorescent dye that has been widely used to measure cell death by assessing plasma membrane integrity with flow cytometry.[38] In combination with a nuclear stain, it can also be used in automated microscopy.[39,40] Our PI Cytotoxicity Assay (*Fig. 1A*, right panel) uses just PI and can be read on a fluorescence plate reader, which allows for higher throughput.

After compound treatment, dead cells are labeled with PI giving a red fluorescence that is proportional to the amount of dead cells in the well. After the first fluorescence measurement, a solution of 0.8% Triton X-100 is added to permeabilize and label all cells in the well. The PI fluorescence is then measured again to obtain a value that is now proportional to the total amount of cells present in each well. This ratiometric assay allows us to calculate the proportion of cell death induced by the compound treatment (*Fig. 1A*) eliminating the variations that can arise from a different number of cells per well and/or different growth rates resulting from compound treatment.

To evaluate the performance of our PI Cytotoxicity Assay, we determined the LC_{50} of siramesine, a well-characterized LCD inducer, on the human breast cancer cell line MCF7 after 24 h of exposure.[25] Siramesine is not commercially available and was synthesized in our laboratory following the protocol described in Materials and Methods (*Supplementary Fig. S1*).

Using our PI-Cytotoxicity Assay we found an LC_{50} of 33.2 ± 2.8 μM (*Fig. 1B, C*). This LC_{50} is higher than the previously published values, but the difference can be attributed to experimental conditions, mainly the higher cell density, which affects siramesine sensitivity.[20] The method is highly reproducible, since we obtained similar LC_{50} values for siramesine in five independent experiments. These results illustrate the utility of our assay and, in addition, confirm the cytotoxicity of our newly synthesized siramesine. Importantly, no washing step is required, making the assay amenable to HT applications.

In a pilot experiment in the 96-well format using siramesine (30 μM, positive control) and 0.5% DMSO (negative control), the assay gave an 80-fold S/N, which is more than sufficient for a HTS assay. The Z′ factors measured in five independent plates were 0.8–0.95, with a mean of 0.86 (data not shown) indicating a robust and reliable assay.[37]

To distinguish between compounds that are able to trigger alternative cell death pathways and those that can only induce apoptosis, we combined our PI Cytotoxicity Assay with MCF-7 cell lines genetically modified to have differential sensitivities to apoptosis inducers; (1) MCF7 cells that overexpress Bcl2 protein (MCF7-Bcl2) and are highly resistant to apoptotic cell death;[35] (2) The parental MCF7 cells (MCF-wt) that lack functional caspase-3 due to a 47-base pair deletion within exon 3 of the caspase 3 (*CASP3*) gene and are partially resistant to apoptotic stimuli;[41] and (3) MCF7 cells that overexpress wild-type caspase-3 (MCF7-Casp3) and therefore have fully restored apoptotic signaling.[20] Only compounds that act through nonapoptotic pathways are expected to show similar toxicity against all three cell lines. Compounds that trigger apoptosis would be more toxic to MCF7-Casp3 cells and less or nontoxic to MCF7-Bcl2 cells compared to the MCF7-wt cells.

Siramesine showed similar toxicity on all three cell lines (*Fig. 1D*). This is in agreement with the fact that siramesine-induced cell death is Bcl2 insensitive and caspase-3 independent.[25] In contrast, the three cell lines showed very distinct responses to staurosporine, an inducer of classical apoptosis: MCF7-Bcl2 cells were completely resistant in the tested concentration range, MCF7-wt cells were partially resistant, and MCF7-Casp3 cells were highly sensitive, the expected profile for a drug inducing classical apoptosis (*Fig. 1E*). These results demonstrate that the MCF7-Bcl2 cell line can be used in a primary screen to discriminate between compounds that induce apoptosis (staurosporine) and those that trigger Bcl2-insensitive and caspase-3-independent alternative cell death pathways such as LCD (siramesine).

A HTS Assay Identified 39 Small Molecules That Induced Bcl2- and Casp3-Independent Cell Death in Cancer Cells

We used MCF7-Bcl2 cells to screen the Prestwick Chemical library (Prestwick Chemical, France), composed of 1,280 Food and Drug Administration (FDA)-approved off-patent compounds. The compounds were screened at a final concentration of 50 μM, and cytotoxicity was measured after 24 h using our PI Cytotoxicity Assay. Compounds that induced more than 10% cell death were selected as hits for retesting. The threshold was set based on the mean response of the negative control across the screening campaign plus three SDs.[37] Siramesine was used as a positive control and the apoptosis inducer staurosporine was also included.

The Z′-factor was calculated for each screened plate from the controls and was >0.5 in all cases.[37] The results of the

Table 4. Cytotoxicity Screening Hits

Compd.[a]	Compd. Name	Primary Screening	Dose–Response Confirmation		U2OS-mCherry-Gal-3 Reporter Assay		Activity Characteristics
		McCF7-Bcl2% Dead Cells at 50 μM[b]	MCF7-Bcl2 LC_{50} μM[c]	MCF7-Casp3 LC_{50} μM[d]	Optimal Concentration μM[e]	Mean Gal-3 Puncta Area Per Cell[f]	
Structural group 1. Promazine derivatives							
1	Triflupromazine HCl	61.5	43.2 ± 4.4	44.1 ± 4.5	23	9.8 ± 7.7	ASM, CAD, LCD
2	Chlorpromazine HCl	11.2	42.9 ± 3.0	46.0 ± 1.9	23	9.5 ± 4.3	LT, ASM, CAD, LCD
3	Thioridazine HCl	101.1	20.3 ± 4.1	22.0 ± 1.8	23	24.5 ± 1.4***	LT, ASM, CAD
4	Perphenazine	100.2	26.3 ± 1.8	35.1 ± 8.4	30	31.0 ± 12.8***	ASM, CAD
5	Trifluoperazine diHCl	100.1	22.1 ± 4.3	29.7 ± 6.2	30	46.6 ± 9.8***	ASM, CAD, LCD
6	Fluphenazine diHCl	100.1	26.5 ± 1.3	26.3 ± 2.8	23	44.7 ± 12.2***	ASM, CAD, LCD
7	Prochlorperazine dimaleate	73.9	27.4 ± 1.0	29.9 ± 4.0	23	12.9 ± 8.7	CAD
8	Methixene HCl	23.6	35.0 ± 8.0	34.4 ± 7.1	30	13.1 ± 1.0	CAD
9	Trimeprazine Tartrate[g]	5.3	>60	>60	30	4.0 ± 1.1	CAD
10	Zuclopenthixol HCl	54.2	40.6 ± 3.7	34.6 ± 9.2	30	19.8 ± 7.2*	CAD
11	Thiethylperazine malate	60.7	20.1 ± 4.9	23.8 ± 1.0	23	29.6 ± 9.6***	CAD
12	Thioproperazine dimesylate	52.9	38.3 ± 3.7	46.4 ± 9.1	30	66.6 ± 0.1***	CAD
13	Chlorprothixene HCl	31.1	41.4 ± 2.9	44.8 ± 3.2	30	10.3 ± 8.3	ASM, CAD
14	Acetopromazine Maleate Salt[g]	0.25	>60	>60	30	2.8 ± 1.5	CAD
15	Promazine HCl[g]	0.22	>60	>60	30	3.7 ± 2.9	ASM, CAD
16	Methotrimeprazine	38.9	43.0 ± 7.2	44.5 ± 3.4	23	7.6 ± 4.1	CAD
17	Piperacetazine[g]	0.26	>60	>60	30	11.0 ± 9.0	CAD
Structural group 2. Tamoxifen and derivatives							
18	Tamoxifen Citrate	54.5	36.2 ± 7.2	37.0 ± 1.3	23	31.9 ± 8.2***	LCD, ASM, CAD
19	Clomiphene Citrate (Z,E)	10.5	31.6 ± 7.9	34.0 ± 8.1	23	39.9 ± 0.2***	ASM, CAD
20	Toremifene	100.8	36.2 ± 10.2	45.5 ± 10.9	30	29.7 ± 6.5***	CAD
Structural group 3. Siramesine like compounds							
21	Astemizole	91.0	15.3 ± 1.0	31.3 ± 1.6	8	87.7 ± 10.9***	LT, ASM, CAD
22	Sertindole	100.5	22.5 ± 7.0	24.3 ± 3.5	18	102.4 ± 10.7***	ASM, CAD
Structural group 4.							
23	Mefloquine HCl	103.1	21.6 ± 3.1	21.4 ± 2.5	14	39.6 ± 7.8***	LCD, CAD
24	Primaquine diphosphate[g]	8.6	>60	>60	30	8.6 ± 0.5	

(*continued*)

Table 4. *Continued*

Compd.[a]	Compd. Name	Primary Screening	Dose–Response Confirmation		U2OS-mCherry-Gal-3 Reporter Assay		Activity Characteristics
		McCF7-Bcl2% Dead Cells at 50 μM[b]	MCF7-Bcl2 LC_{50} μM[c]	MCF7-Casp3 LC_{50} μM[d]	Optimal Concentration μM[e]	Mean Gal-3 Puncta Area Per Cell[f]	
Structural group 5.							
25	Terfenadine	105.1	13.5 ± 1.0	13.9 ± 2.5	8	51.1 ± 2.9***	LCD, ASM, CAD
Structural group 6.							
26	Chlorhexidine	106.1	14.2 ± 1.0	12.5 ± 2.2	8	3.1 ± 1.8	
27	Alexidine diHCl	98.8	7.9 ± 2.0	6.2 ± 1.0	5	1.135 ± 0.9	
Structural group 7.							
28	Fendiline HCl	52.7	36.8 ± 5.4	32.2 ± 3.3	23	37.2 ± 2.6***	ASM, CAD
29	Pimozide	59.6	34.8 ± 4.5	39.2 ± 3.9	23	59.4 ± 10.8***	ASM, CAD
30	Fluoxetine HCl	32.6	47.2 ± 1.8	63.2 ± 8.2	30	45.1 ± 13.9***	LT, ASM, CAD
31	Prenylamine lactate	70.7	25.1 ± 5.5	20.1 ± 3.7	11	17.6 ± 6.8	CAD
32	Fluspirilene	58.6	25.4 ± 3.6	29.9 ± 1.0	14	40.2 ± 7.6***	CAD
33	Loperamide HCl[g]	2.0	>60	>60	30	29.2 ± 1.4***	CAD
34	Flunarizine diHCl[g]	1.23	>60	>60	30	4.2 ± 0.2	CAD
35	Lidoflazine	48.2	28.8 ± 2.0	30.9 ± 4.9	14	34.7 ± 1.9***	CAD
36	GBR 12909 diHCl[g]	0.1	>60	>60	30	21.6 ± 5.2**	CAD
Structural group 8.							
37	Methyl benzethonium chloride	100.5	16.6 ± 4.3	13.3 ± 3.6	8	6.0 ± 1.9	
38	Benzethonium chloride	88.9	15.5 ± 1.0	14.2 ± 1.3	8	7.5 ± 4.9	
39	Thonzonium bromide	108.1	12.4 ± 1.3	7.2 ± 1.0	6	10.0 ± 5.5	
Structural group 9.							
40	Perhexiline maleate	105.0	17.9 ± 2.2	16.8 ± 3.9	14	76.9 ± 10.8***	ASM, CAD
41	Metergoline	105.1	34.5 ± 7.0	37.7 ± 5.2	23	36.1 ± 2.7***	
42	Amethopterin (R,S)[g]	7.4	>60	>60	30	3.8 ± 0.7	
43	Methotrexate (L)[g]	0.8	>60	>60	30	4.3 ± 1.8	
44	Suloctidil	109.1	18.1 ± 2.2	17.7 ± 4.7	6	41.2 ± 10.3***	ASM CAD
45	Parthenolide	40.8	24.8 ± 3.6	30.5 ± 6.9	18	20.0 ± 0.4**	
46	Cilostazol[g]	0.32	>60	>60	30	4.4 ± 0.5	
47	Beta-Escin	87.5	18.8 ± 1.7	25.9 ± 1.3	11	6.7 ± 0.6	

(*continued*)

Table 4. *Continued*

Compd.[a]	Compd. Name	Primary Screening	Dose–Response Confirmation		U2OS-mCherry-Gal-3 Reporter Assay		Activity Characteristics
		McCF7-Bcl2% Dead Cells at 50 μM[b]	MCF7-Bcl2 LC_{50} μM[c]	MCF7-Casp3 LC_{50} μM[d]	Optimal Concentration μM[e]	Mean Gal-3 Puncta Area Per Cell[f]	
48	Thimerosal	93.1	18.4 ± 2.1	12.3 ± 6.4	11	11.5 ± 2.6	
49	Auranofin	109.0	6.5 ± 1.9	8.8 ± 1.0	5	11.8 ± 2.3	
50	Sertraline	105.1	28.8 ± 1.3	27.3 ± 1.4	18	22.4 ± 1.8**	LT, ASM, CAD
Controls							
SIRA	Siramesine	99.3 ± 8[h]	35.1 ± 3[i]	36.2 ± 4[i]	23	40.5 ± 7.7***	LT, LCD, ASM
STAU	Staurosporine	0.83 ± 2[h]	>60	5.7 ± 3	4	8.3 ± 4.2	
DMSO	DMSO 0.5%	0.2	–	–	–	5.3 ± 1.6	

[a]Compound number is as in *Figure 2*.
[b]Percentage of cell death on MCF7-Bcl2 cells obtained in the primary screening (*Fig. 1F*).
[c–d]LC_{50} ± 95% CI calculated from a best-fit curve with a nonlinear regression with Graph Pad Prism 5.0. An LC_{50} > 60 means that the compound did not show activity at the measured concentration range. See the LC_{50} curves in *Supplementary Figures S2 and S3*.
[e]Correspond to the concentration that showed highest spot area per cell with minimum cell death.
[f]Average ± SD (n = 2) of "Mean_SpotAreaPerObject." Asterisks indicate statistical difference with respect to Staurosporine (negative control). The P values expressed as: *** <0.001, **0.001–0.01, *0.01–0.05 (two tailed, equal variance t-test). Values are plotted in *Figure 5B*.
[g]Compounds that showed no activity in the primary screening, but were selected to follow-up due to its structural similarities with the hits.
[h]The positive and the negative control were present in all the screening plates in five replicates. The value shown here is the average ± SD between all screening plates.
[i]Siramesine dose–response curve was included in all the screening plates to assess variability between the plates. The value shown here is the mean ± SD of nine curves across the screening plates.
95% CI, 95% confidence interval; ASM, acid sphingomyelinase; CAD, cationic amphiphilic drug; Casp3, caspase 3; Gal-3, galectin-3; SD, standard deviation; LCD, lysosomal cell death; LT, lysosomotropic.

primary screening are summarized in *Figure 1F*. Fifty compounds were selected as follows: (1) 39 compounds (3% of the library) induced more than 10% cell death in MCF7-Bcl2 cells and were consider as Hits. (2) The other 11 compounds showed low potency (<10%) but had chemical structures closely related to the Hits. These compounds were also selected to further confirm their lack of cytotoxicity and to serve as internal controls in our characterization. The structures of the 50 selected compounds are shown in *Figure 2*, and *Table 1* summarizes the percentages of dead cells for these compounds.

To confirm that the cytotoxicity of the 39 hits was caspase-3 independent, we established and compared their LC_{50} in MCF7-Bcl2 and MCF7-Casp3 cells using eight different concentrations

Fig. 3. LC_{50} values of Prestwick Library Hits in MCF7-Casp3 and MCF7-Bcl2. MCF7-Casp3 and MCF7-Bcl2 cells were exposed to the 50 compound selected in the primary screen. Cells were treated with eight different concentrations for 24 h, and cell death was measured with the HT *PI Cytotoxicity Assay*. The percentage of dead cells (mean ± SD, n = 3) was used to calculate the LC_{50} values. **(A)** Each point represents the calculated LC_{50} ± 95% CI for each compound on both cell lines. The *solid black line* corresponds to an artificial line with slope = 1, representing the ideal situation where the LC_{50} is identical on both cell lines. (*Green circle*) LC_{50} for siramesine calculated from nine dose–response curves distributed across the screen plates; (*blue circle*) LC_{50} for staurosporine; (*black circle*) LC_{50} for Prestwick library Hits; (*red circle*) LC_{50} for Prestwick library Hits for which dose–response curves are showed in D. Thirty-five out of 39 Hits showed similar LC_{50} in both cell lines (F-test, P > 0.05), suggesting that cell death induced by most of the hits is indeed Casp3 and Bcl2 independent. **(B)** Dose–response curves for siramesine (mean of nine curves) in MCF7-Bcl2 (*blue diamond*) and MCF7-Casp3 (*red circle*). Siramesine showed similar LC_{50} in both cell lines (F-test, P = 0.52). **(C)** Dose–response curves for staurosporine in MCF7-Bcl2 (*blue diamond*) and MCF7-Casp3 (*red circle*). **(D)** Dose–response curves for representative compound in MCF7-Bcl2 (*blue diamond*) and MCF7-Casp3 (*red circle*). F-test shows no significant difference ($P \geq 0.05$). In all cases, each data point is the mean ± SD (n = 3), and the LC_{50} ± 95% CI was calculated from a best-fit curve with a nonlinear regression model using GraphPad Prism 5.0 software. Comparison of LC_{50} was made through an F-test with GraphPad Prism 5.0 software. When P > 0.05, the LC_{50}s were considered not significantly different. The dose–response curves for all compounds tested during the confirmation screening are shown in *Supplementary Figures S2* and *S3*.

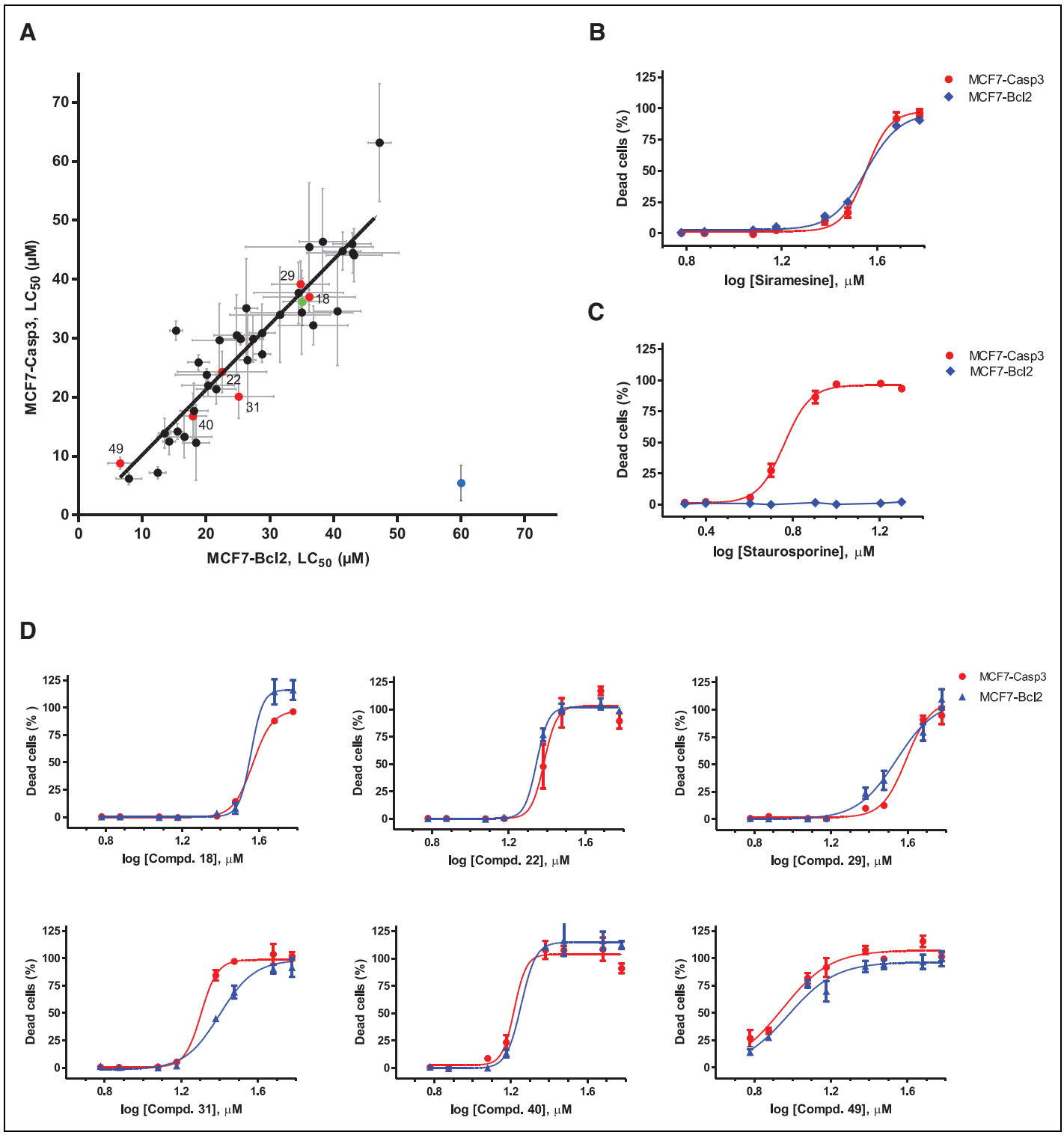
A
MCF7-Casp3, LC50 (μM)
MCF7-Bcl2, LC50 (μM)
29
18
22
31
40
49
B
Dead cells (%)
log [Siramesine], μM
MCF7-Casp3
MCF7-Bcl2
C
Dead cells (%)
log [Staurosporine], μM
MCF7-Casp3
MCF7-Bcl2
D
Dead cells (%)
log [Compd. 18], μM
log [Compd. 22], μM
log [Compd. 29], μM
log [Compd. 31], μM
log [Compd. 40], μM
log [Compd. 49], μM
MCF7-Casp3
MCF7-Bcl2

ranging from 6 to 60 μM. The 39 hits induced dose-dependent cytotoxicity in MCF7-Bcl2 cells and MCF7-Casp3 cells (*Table 4* and *Supplementary Figs. S2* and *S3*). We found that 35 out of 39 hits showed a similar LC_{50} in both cell lines (F-test, $P > 0.05$), suggesting that cell death induced by these compounds is caspase3 independent (*Fig. 3*). On the contrary, staurosporine showed a low micromolar LC_{50} in MCF7-Casp3 cells and no cytotoxicity against MCF7-Bcl2 cells up to 60 μM. Most of the hits had a lower LC_{50} than siramesine, the most potent hit being auranofin (compd. 49).

The success of our approach was validated by the identification of some previously described LCD inducers such as tamoxifen (compd. 18)[42,43] and terfenadine (compd. 25).[42,43,44] Moreover, the 11 structurally related compounds that showed no activity in the primary screening were confirmed as inactive against both cell lines in this concentration range (*Table 4* and *Supplementary Figs. S2* and *S3*), thus confirming their lack of cytotoxicity and ruling out possible false negatives in our assay.

Inspection of chemical structure similarities revealed that the hits could be classified in nine different structural groups (*Fig. 2* and *Table 4*). The largest group of compounds, group 1, includes 17 phenothiazine derivatives, many of which are tricyclic antidepressants and antipsychotics. Some phenothiazine derivatives have previously been described to accumulate in lysosomes and induce LCD (*Table 4*, LCD).[45] Importantly, we notice that many of our hits are lipophilic and contain an amine group with a pKa >6 (*Supplementary Table S1*). This resembles the physicochemical properties of the so-called CADs (*Table 4*), which are known to accumulate in the lysosome.[23] In fact, at least six of our hits have previously been shown to do so[23] (*Table 4*, lysosomotropic [LT]). Interestingly, 19 compounds have been shown to inhibit acid sphingomyelinase (ASM, *Table 4*).[46] Both the accumulation of compounds in the lysosomes and their ability to inhibit ASM have been shown to be related to LCD induction.[25,35,44] Group 9 includes a variety of structurally unrelated compounds, many of which have not been described before to induce an alternative cell death pathway.

An HT Image-Based Assay Classified 24 Compounds as LCD Inducers

We developed an HT image-based assay that can reliably measure LMP, the main hallmark of LCD, to determine which of our hits actually killed through LCD. Many groups have used fluorescent dyes such as LysoTracker Red-DND-99 or Acridine Orange to measure lysosomal membrane damage. These methods rely on the pH gradient between the lysosome (4.6–5.0) and the cell cytosol (around neutral).[24,47,48] However, most of the identified LCD inducers were LT compounds, comprising basic CADs. These drugs accumulate in the lysosomes as they get protonated, significantly increasing the lysosomal pH and competing with the dyes. This phenomenon results in a pH-dependent decrease in the fluorescence signal of the above-mentioned dyes, without necessarily indicating LMP.[24] In fact, many of our 11 structurally related nonactive compounds showed complete depletion of LysoTracker-Red florescence after 2–4 h of exposure (*Supplementary Table S1*), despite having no cytotoxic effect. This clearly indicates that pH-dependent dyes should not be used to measure LMP.

As an alternative, we developed an assay using the Gal-3 reporter system, which has been previously used as a marker of vacuole lysis by invasive pathogens and that we have used to detect LMP induced by various stimuli.[27–29,32] To generate a reporter cell line that expresses Gal-3 in the cytosol, we fused Gal-3 protein to a monomeric green fluorescent protein (mAG-Gal3) with which we stably transfect MCF7-Bcl2 cells. MCF7-Bcl2-mAG-Gal3 cells expressed cytosolic mAG-Gal3 protein with a diffuse homogenous phenotype. Upon treatment with siramesine for 6 h, mAG-Gal3 formed a punctate pattern (*Fig. 4A*). The location of the puncta around the nuclei suggested that these structures corresponded to damaged lysosomes to which mAG-Gal3 had translocated. The punctate pattern was not observed when cells were treated with staurosporine for 6 h, which instead showed a dispersed mAG-Gal3 pattern, similar to the untreated cells, and apoptotic membrane blebbing (*Fig. 4A*).

To confirm that mAG-Gal3 dots indeed corresponded to lysosomes with a damaged membrane, MCF7-Bcl2-mAG-Gal3 cells were treated with siramesine for 6 h and stained with LysoTracker Red-DND-99 (*Fig. 4B*). Vesicles with intense mAG-Gal3 fluorescence were negative for LysoTracker, indicating membrane damage. The vesicles that still retained LysoTracker were either negative for mAG-Gal3 or showed weak staining, suggestive of partial leakage.[26,32] Similar phenotypes were observed with a second reporter cell line, U2OS cells stably transfected with m-Cherry-Gal3 plasmid (U2OS-mCherry-Gal3, *Fig. 4C*).

We used U2OS-mCherry-Gal3 reporter cell line to develop a rapid cell-based HT assay to measure lysosomal leakage in live cells. The U2OS-mCherry-Gal3 cells were preferred because the low expressions of exogenous mCherry-Gal3 in these cells make them more suitable for the detection of Gal-3 puncta using a widefield automated microscope. After compound treatment, the bright mCherry-Gal3 puncta that formed were easily distinguished from the faint cytosolic fluorescence background of the mCherry-Gal3 still remaining in the cytosol. On the contrary, MCF7-Bcl2-mAG-Gal3 expressed a high amount of mAG-Gal3; thus, although mAG-Gal3 spots were visible, they were difficult to discriminate from the still bright cytosolic fluorescence background. Therefore, U2OS cells were

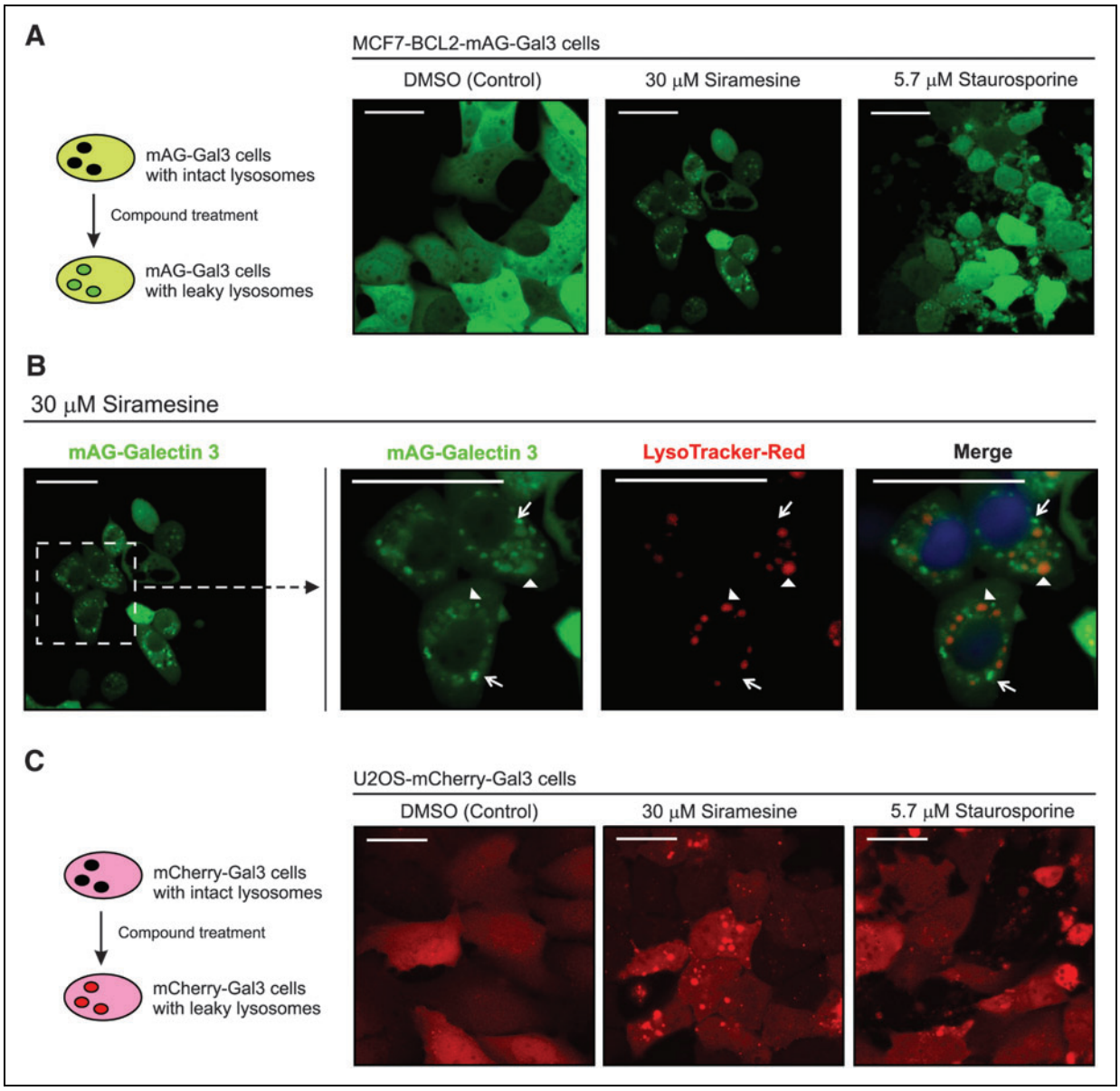

Fig. 4. Detection of LMP with Galectin-3 reporter cell lines. **(A)** *Left panel:* Schematic representation of the mAG-Gal3 reporter assay. MCF7-Bsl2 cells express mAG tagged Gal-3 protein in the cytosol and contain intact lysosomes (*black vesicles*). After compound treatment, the permeabilization of the lysosomal membrane allows the entry of the cytosolic expressed mAG-Gal3 protein, resulting in bright fluorescent spots (permeabilized lysosomes, *green vesicles*). *Right panel:* Confocal images of MCF7-Bcl2-mAG-Gal3 cells, after treatment for 6 h as indicated. **(B)** MCF7-Bcl2-mAG-Gal3 cells were treated with 30 μM siramesine for 6 h and then stained with LysoTracker Red-DND-99 to mark the intact lysosomes. *Right panel:* Zoom-in of the indicated area showing the single channel images for mAG-Gal3 and LysoTracker-Red, and merge. The *arrows* pointed to damaged lysosomes that showed strong Gal-3 stain and were negative LysoTracker. The *arrowheads* point to lysosomes that have not totally released their content yet, showing LysoTracker staining and deem stain for mAG-Gal3. **(C)** *Left panel:* Schematic representation of the mCherry-Gal3 reporter assay. The principle is as in **(A)**. *Right panel:* Confocal images of U2OS-mCherry-Gal3 cells, after treatment for 6 h with the indicated compounds. In all images, scale bars = 50 μm. Data shown are representative images of three independent experiments. Gal-3, galectin-3; LMP, lysosomal membrane permeabilization.

chosen for the phenotypic HT assay development, and the Gal-3 puncta were recognized by automated microscope as "spots."

Calcein-AM, which is only fluorescent in metabolically active cells, was used to guarantee that only live cells were taken into account in the quantification of m-Cherry-Gal3 puncta. The fluorescent dye, Hoechst 33342, was used to stain nuclei. U2OS-mCherry-Gal3 cells were treated for 6 h with serial dilutions (10 concentrations, 3–30 μM) of the 50 compounds selected in the primary screen. The selection of a 6-h treatment was based on time course confocal microscopy experiments, in which 6 h was the optimum time to detect abundant mCherry-Gal3 puncta while cells remained still viable as judged by their morphology and Calcein-AM stain (data not shown). Automated live-cell image acquisition was performed with a Thermo Cell Insight™ HCS reader, and the quantification algorithm was optimized to detect mCherry-Gal3 puncta.

In this algorithm, cells were first identified by their nuclear stain and a circular region for each cell was defined centered in the nucleus. Gal-3 intense fluorescent areas (spots) within this circular region were identified and analyzed (*Fig. 5A*). In our assay, these spots represent the Gal-3 that has translocated to damage lysosomes and was quantified as the "Mean_SpotAreaPerCell (MSAPC)" in channel 2. Special attention was taken to avoid the identification and quantification of cell blebbing, observed with apoptosis inducers like staurosporine, as mCherry-Gal3 puncta (see Materials and Methods). A punctate pattern of mCherry-Gal3 was observed in samples treated with 23 μM siramesine (*Fig. 5A*). The quantification of 10 random fields in duplicate samples showed a mean MSAPC of $40.5 \pm 7.7\ \mu m^2$ (*Table 4*). Significantly less Gal-3 puncta were detected in samples treated with DMSO or staurosporine (*Fig. 5A*) with a mean MSAPC of 5.3 ± 1.6 and $8.3 \pm 4.2\ \mu m^2$, respectively. Hence, the image-based assay was able to correctly identify siramesine as an LCD inducer compound and staurosporine as a non-LCD inducer based on the total area occupied by bright mCherry-Gal3 puncta after treatment.

The distinction between the controls was significant throughout the screening plates, with calculated Z′-factors for individual plates ranging from 0.39 to 0.7, and S/B was 10 across all plates. We tested all compounds in dose–response, with eight concentrations ranging from 3 to 30 μM. Active compounds showed a dose-dependent increase of mCherry-Gal3 puncta, but the highest concentration(s) induced extensive cell death with cell rounding up, which hampered the mCherry-Gal3 spot quantification (*Supplementary Fig. S4*). Nevertheless, an optimal concentration could be identified for each compound, at which the mCherry-Gal3 puncta were clearly visible and abundant with low cell cytotoxicity. Due to the different potency of the hits, the optimal concentration varied across all 50 tested compounds (*Supplementary Figs. S4–S6*). Thus, for this type of image-based phenotypic assay, it is advantageous to screen all compounds in dose–response instead of simply using a single screening concentration.

The mean of MSAPC of mCherry-Gal3 puncta at the selected optimal concentration for each compound was extracted from the dose–response curves and compared with that of the staurosporine control to determinate if the observed increase in mCherry-Gal3 puncta area was statistically significant ($P < 0.05$, *t*-test), thus defining if a compound induced lysosomal leakage (*Fig. 5B* and *Table 4*). Of the 39 hits identified in the primary screen, 24 (>50%) induced strong mCherry-Gal3 puncta formation at 6 h and were identified as LCD inducers (*Table 4* and *Fig. 5B*). Most of these compounds were CADs, but the assay was also able to identify a non-CAD as LCD inducer, parthenolide (compd. 45). The remaining 15 compounds, which were able to kill apoptosis-resistant cells, showed no mCherry-Gal3 puncta development, indicating a different mechanism than LCD. Among these were the five compounds of the structural groups 6 and 8 (compds. 26–27 and 36–38), which most likely kill nonspecifically due to detergent properties.

Several phenothiazine hits (group 1, compds. 1, 2, 7, 8, 13, and 16) failed to induce the formation of mCherry-Gal3 puncta (*Table 4* and *Supplementary Fig. S5*). Instead, they

Fig. 5. Quantification of Gal-3 relocalization to damaged lysosomes by automatic microscopy. LMP can be detected in U2OS-mCherry-Gal3 reporter cells using an automatic microscope. Cells were treated for 6 h, at concentrations between 3 and 30 μM. Cells were stained with Hoechst (nuclear mask) and Calcein-AM (cell mask) and subjected to quantitative image analysis using the CellInsight™ CX5 high content screening (HCS) Platform. The quantification algorithm was optimized to detect the mCherry-Gal3 puncta (damaged lysosomes) within a mask. mCherry-Gal3 puncta were quantified as the Mean_SpotAreaPerCell in channel 2. **(A)** CellInsight representative images for siramesine, the negative controls (DMSO and staurosporine) and two example compounds. Images for the single channels and the merge are presented. At the most *right side* we show the mCherry-Gal3 (*white*) in overlay with the quantification marks for "nucleus" (*blue*), "cell mask" (*green*), and "detected spots" (*yellow*) as defined by the established automatic cell image quantification algorithm (*Table 3*). **(B)** Mean ± SD ($n = 2$) of "Gal-3 Mean_SpotAreaPerCell" for the 50 compounds tested (*black bars*) and mean ± SD ($n = 135$, across plates) for siramesine (*green bar*), staurosporine (*red bar*), and the vehicle (DMSO, *gray bar*). For the 50 compounds, the values presented correspond to the results at the optimal concentration extracted from the dose–response curves (*Table 4* and *Supplementary Figures S5* and *S6*). Compound number relates to *Figure 2*. On each well, 10 images with a total of >500 cells/sample were quantified. *Asterisks* indicate statistical difference with respect to staurosporine (*red bar*), with *P* values expressed as ***$P < 0.001$, **$P = 0.001$–0.01, and *$P = 0.01$–0.05 (two tailed, equal variance *t*-test).

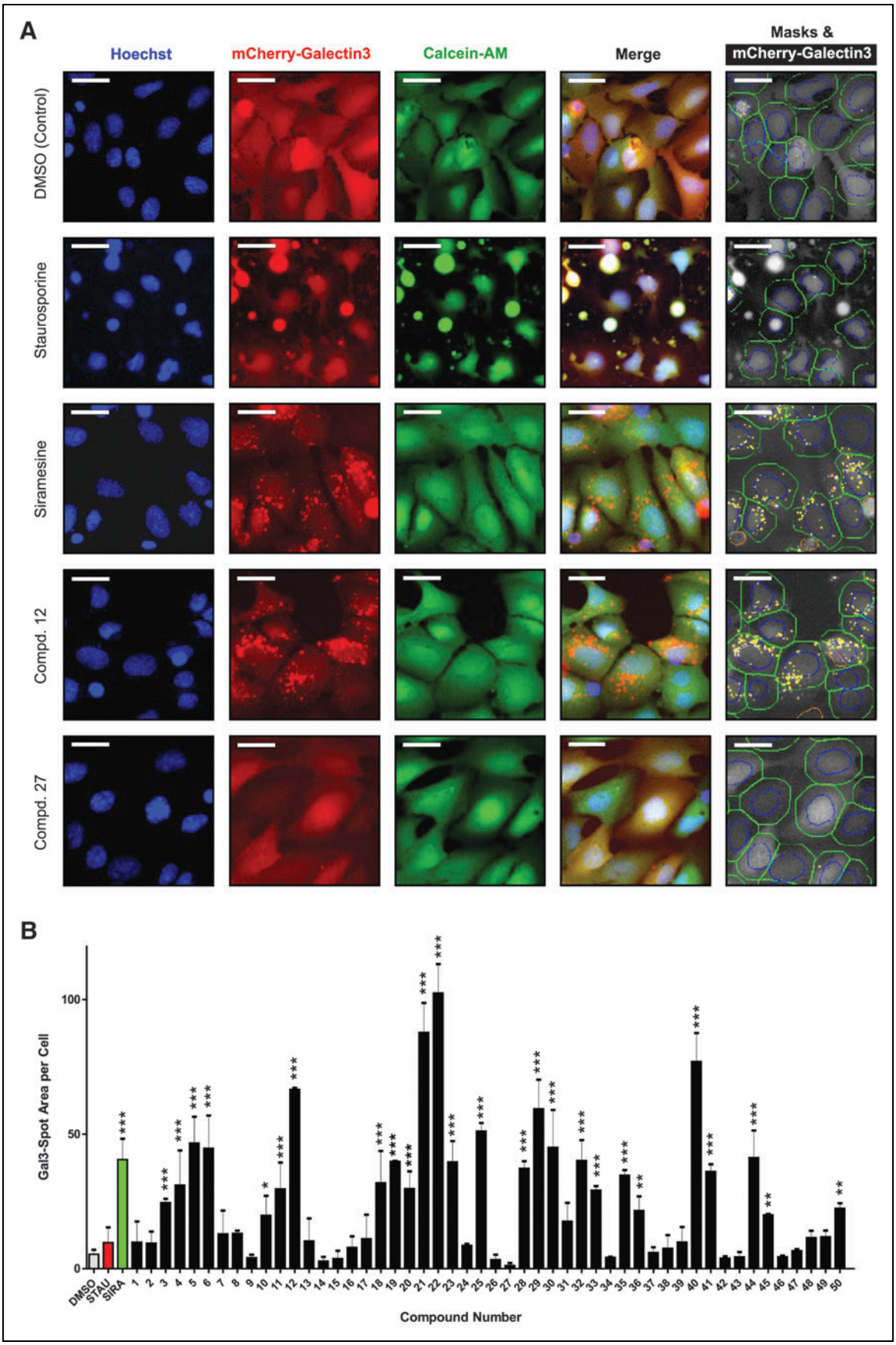
A
Hoechst
mCherry-Galectin3
Calcein-AM
Merge
Masks &
mCherry-Galectin3
DMSO (Control)
Staurosporine
Siramesine
Compd. 12
Compd. 27
B
Gal3-Spot Area per Cell
100
50
0
DMSO
STAU
SIRA
1 2 3 4 5 6 7 8 9 10 11 12 13 14 15 16 17 18 19 20 21 22 23 24 25 26 27 28 29 30 31 32 33 34 35 36 37 38 39 40 41 42 43 44 45 46 47 48 49 50
Compound Number

caused the cells to quickly round up, without blebbing or nuclear condensation, suggesting a type of cell death that is neither apoptosis nor LCD. Importantly, these phenothiazine derivatives decreased LysoTracker staining after 4 h, indicating that they do accumulate in lysosomes (*Supplementary Table S1*).

Moreover, the 11 structurally related compounds that did not induce cell death in the primary screen (*Table 4*) also failed to induce mCherry-Gal3 puncta, except loperamide and GBR 12909 (compds. 33 and 36). Importantly, most of them did alter LysoTracker staining due to its CAD properties (*Supplementary Table S1*) while our Gal-3 assay was not affected by their basic properties as CADs. Therefore, LysoTracker-Red assay incorrectly identifies as an LCD inducer any compound with CAD properties, even if they are not cytotoxic (*e.g.*, compd. 14, *Fig. 6A*) or if they are cytotoxic but do not damage the lysosomal membrane (*e.g.*, compd. 16, *Fig. 6A*). Thus, this confirms that the Gal-3 reporter assay can discriminate between compounds that induce LMP and those that merely affect the pH of the lysosome but do not permeabilize its membrane. This clearly shows the advantages of the Gal-3 assay against using assays based on LT dyes (*e.g.,* LysoTracker-Red).

Finally, the identification of a non-CAD LCD inducer and the fact that some CADs showed no Gal-3 puncta, despite its accumulation in lysosomes, suggest that the accumulation in lysosomes might be important but not sufficient to induce LCD.

Since one of the major hallmarks of LCD is the release of cathepsins to the cytosol, we compared the Gal-3 assay with the detection of cathepsins in the cytosol by immunostaining for three randomly selected compounds classified as LCD inducers in our phenotypic assay (*Fig. 6B*). Immunostaining of cathepsin D showed a change of pattern from punctate to a more diffuse cytosolic and nuclear staining upon 6-h treatment with siramesine and three selected LCD inducer compounds (*Fig. 6B*). Importantly, cell death induced by these compounds was not decreased by preincubation of cells with either a pan-caspase inhibitor or an inhibitor of necroptosis (*Supplementary Fig. S7*).

All together this demonstrates that our platform can be used to successfully identify inducers of LCD.

DISCUSSION

The aim of our study was to develop a rapid screening platform for the identification of compounds that induce LCD. We settled upon a two-step strategy. First, a primary screen was used to identify compounds that induce alternative PCD while rapidly eliminating the compounds that induce classical apoptosis. A secondary image-based screen was used to identify those hits from the primary screen that specifically induced LCD.

Our primary screen, a ratiometric assay based on nuclear PI uptake in MCF7-Bcl2 cells, allowed us to rapidly eliminate compounds that only kill through canonical apoptotic pathways. The assay is simple, inexpensive, fast, and very reproducible. It can be read on a fluorescence plate reader, making it suitable for HT testing of 100,000s of compounds in a short period of time. One major advantage of this assay is that it measures cell death directly. Many commonly used cell viability assays, such as CellTiter-Glo (Promega), measure metabolism, which can vary independently of toxicity. These assays cannot distinguish between cytotoxicity and inhibition of proliferation.

Our assay has the advantage of measuring cytotoxicity independently of metabolism and proliferation, as it calculates the percentage of cell death in relation to the total cell content of each well. The assay can be performed in complete media, allowing for more prolonged compound exposure times than buffer-based systems, and it requires no washing steps, which makes it amenable to automation. A major advantage of using a genetically modified apoptosis-resistant cell line is that there is no need to introduce a pretreatment

Fig. 6. The Gal-3-based LMP assay can better discriminate between compounds that induce LMP and those that merely affect the pH of the lysosome, but do not permeabilize its membrane. **(A)** *Left panel:* Representative confocal images of MCF7-Bcl2 cells treated for 4 h with vehicle (0.5% DMSO), or a concentration equal to the LC_{50}, of the indicated compounds. Nuclei are visualized with Hoechst 33342 (*blue*), and cells were stained with LysoTracker-Red (*red*). Compounds with negative LysoTracker staining are considered positive for LMP. *Right panel:* Representative confocal images of U2OS-mCherry-Gal3 cells treated for 6 h with vehicle (0.5% DMSO) or the indicated compound at the concentration defined as optimal for Gal-3 puncta quantification (*Table 4*). Nuclei are visualized with Hoechst 33342 (*blue*), and mCherry-Gal3 is shown in *white*. Compounds that Show Gal3 spot pattern are considered positive for LMP. Toxicity (yes/no) indicates if the compound was found to kill MCF7-BCl2 cells in primary screening. CAD (yes/no) indicates if the compound is a CAD. In all images, scale bars = 25 μm. The LysoTracker assay incorrectly identifies all CAD as positive, even when the compound did not show toxicity. On the contrary, the Gal3 assay is not affected by the CAD properties of the tested compound. **(B)** *Left panel:* Representative confocal images of U2OS-mCherry-Gal3 cells treated for 6 h with vehicle, 2.5 μM (staurosporine), 23 μM (siramesine), 23 μM (pimozide, C29), 30 μM (thioproperazine, C12), and 30 μM (trifluoperazine, C5). Nuclei are stained with Hoechst 33342 (*blue*). Lysosomal leakage is visualized by the relocation of Gal-3 to a punctate pattern representing the damaged lysosomes. *Right panel:* Visualization of lysosomal leakage by relocation of cathepsin D from a puncta pattern to a more diffuse cytosolic and nuclear staining. MCF7-Bcl2 cells were treated as in *left panel*, fixed and stained with anti-cathepsin D antibody. In all images, scale bars = 25 μm. CAD, cationic amphiphilic drug.

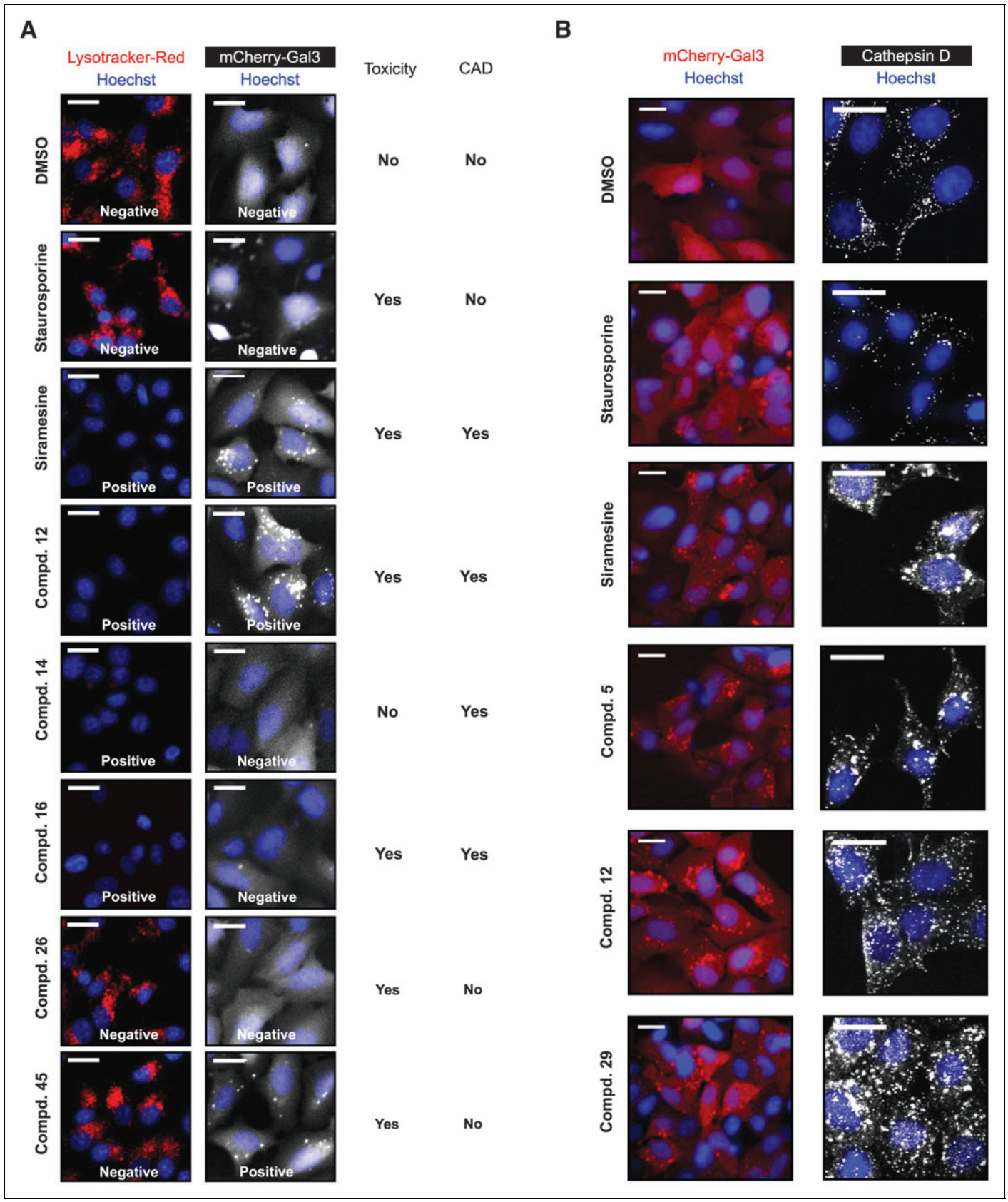
A
Lysotracker-Red
Hoechst
mCherry-Gal3
Hoechst
Toxicity
CAD
DMSO
Negative
Negative
No
No
Staurosporine
Negative
Negative
Yes
No
Siramesine
Positive
Positive
Yes
Yes
Compd. 12
Positive
Positive
Yes
Yes
Compd. 14
Positive
Negative
No
Yes
Compd. 16
Positive
Negative
Yes
Yes
Compd. 26
Negative
Negative
Yes
No
Compd. 45
Negative
Positive
Yes
No
B
mCherry-Gal3
Hoechst
Cathepsin D
Hoechst
DMSO
Staurosporine
Siramesine
Compd. 5
Compd. 12
Compd. 29

with apoptosis inhibitors, which are usually not completely specific, making it necessary to use several inhibitors to obtain reliable results.[49]

Our LMP phenotypic assay based on Gal3 allowed us to identify LCD inducers among the hits from our PI cytotoxicity assay. The assay has a major advantage over previously described methods in that the accumulation of the cytosolic fluorescence-tagged Gal-3 in the damaged lysosomes is completely independent of pH. It depends solely in the permeability of the lysosomal membrane. In this regard, our LMP assay can exclude compounds that accumulate in the lysosomes (*e.g.,* CADs), but do not damage its membrane (*Fig. 6A*). Therefore, our assay minimizes the time consumed during the fruitless analysis of false positives. Furthermore, the assay is simple, rapid, HT, and the use of a second live stain allows us to measure LMP in live cells. The utility of our approach was supported by the identification of five previously described LCD inducers, namely, trifluoperazine (compd. 5), fluphenazine (comp. 6), tamoxifen (compd. 18), terfenadine (compd. 25), and mefloquine (compd. 23).[42–44,50,51]

The mechanisms by which the identified LCD inducers disrupt the lysosomes are unknown. However, like siramesine, most of the hits were CADs (*Table 4*). Astemizole (compd. 21) and sertindole (compd. 22), which show structural features similar to siramesine, were among the compounds with strongest Gal-3 puncta formation, suggesting that they are strong inducers of LCD.[23,46]

As expected, all our hits with CAD properties showed a paid decrease in LysoTracker-Red fluorescence, indicating that they accumulate in lysosomes (*Supplementary Table S1*).[23] It has been suggested that accumulation of compounds in the lysosomes, which can lead to inhibition of ASM, promotes LMP.[23,25,44,46,52] Intriguingly, 9 out of the 31 hits with CAD properties did not show formation of mCherry-Gal3 spots, for example, trifluprom azine (compd. 1), prochlorperazine (compd. 7), methixene (compd. 8), and prenylamine lactate (compd. 31), despite inducing cell death (*Table 4*) and accumulating in lysosomes (*Supplementary Table S1*). Thus, the data suggest that being a CAD, which results in lysosomal accumulation and possibly ASM inhibition, is important but not sufficient to induce LCD.

In agreement with this, our assay was also able to identify a non-CAD LCD inducer, parthenolide (*Fig. 5B*, compd. 45). This compound has no basic group in its chemical structure and it does not accumulate in lysosomes (*Supplementary Table S1*). Therefore, parthenolide must induce LCD by a mechanism independent of lysosomal accumulation. Interestingly, parthenolide (compd. 45) is known to have anticancer activity and has been in clinical trials, but has never before been described as an LCD inducer.[53–56] Nevertheless, it has been shown to increase cysteine protease activity and to induce the appearance of large lysosomal-like structures when used as an antiparasitic, supporting the notion that parthenolide cytotoxicity may be related to lysosomal effects.[57] Parthenolide may affect the lysosomes due to its disruptive effect on microtubules and mitosis.[58,59] Other microtubule-targeting compounds that inhibit the spindle protein Eg5/KIF11 have been shown to cause LMP.[58,59] In addition, parthenolide can lead to the formation of reactive oxygen species that are known to damage lysosomes.[14,60] More experiments are needed to study the mechanism of action of parthenolide and to investigate how LCD can be triggered independently of lysosomal accumulation. It will also be interesting to see whether parthenolide acts synergistically with CADs to induce LCD in cancer cells.

It is surprising to see that from the 39 compounds that were found to induce caspase-3 and Bcl-2-independent cell death in our screen, 24 (61%) were shown to induce LMP/LCD. This supports the notion that LCD is an important alternative cell death pathway that can be exploited for cancer treatment. In cancer cells, the lysosomal compartment is frequently dramatically increased in volume and shows elevated expression and activity of lysosomal enzymes as well as altered membrane trafficking.[61] These changes correlate with the aggressiveness of tumors, but also sensitize cells to LMP.[19,20,62] Therefore, drugs that induce the LCD pathway independently of caspases could be particularly efficient in cancer treatment.[4] This makes our finding that LMP is potentially a common mechanism of action for drugs that kill apoptotic-resistant cells, highly interesting in terms of future drug development. However, anticancer drugs that specifically target this pathway have not yet been developed. This is due at least in part to the limitations of the previously available HT assays that only measure lysosomal accumulation and not LMP. Our platform can contribute to overcome this limitation by allowing the rapid and reliable identification of novel inducers of LCD.

In conclusion, we have demonstrated a robust, HT phenotypic platform that can reliably identify compounds that induce LCD. The assay correctly identified compounds that are known to induce LCD and has also enabled us to identify novel LCD inducers, including parthenolide that represents a novel class of non-CAD LMP/LCD inducers.

Until now, the screening of LCD inducers has been limited by the lack of an HT assay that can differentiate intact from damaged lysosomes while remaining independent of the changes in lysosomal internal pH. The pH dependency of most lysosomal fluorescence stains for live-cell imaging has systematically led to the identification of basic compounds that accumulate in lysosomes as potential LCD inducers (*e.g.,* CADs). Although compound accumulation in lysosomes has been thought to be required for LCD, our assay clearly demonstrates that lysosomal

accumulation is not sufficient or necessary for LCD. Therefore, our HT image-based assay using a Gal-3 reporter provides a useful tool to reliably identify LCD inducers in a technically simple and affordable manner, minimizing false positives and increasing the efficiency of screening campaigns.

The development of anticancer agents with novel mechanisms of action is of key importance in overcoming clinical therapy resistance. The LCD pathway has been suggested as one of this novel potential cancer target, but anticancer drugs that specifically target this pathway are not in clinical use yet.[61] Our data suggest that LMP is potentially a common mechanism of action for drugs that target apoptotic resistant cells. Considering the high frequency of p53 and Bcl2 mutations in human cancer cells, the identification of compounds that induce LMP/LCD could lead to the development of LCD-targeting drugs.

We envisage that our platform can also be used in early preclinical stages to elucidate the role of compound-induced LMP in compound toxicity. Alternatively, it could be incorporated into siRNA knockdown or CRISPR knockout screens to study the molecular mechanism of LCD induction. These could help to gain insight into how different stimuli induce LMP, something that is currently unknown.

ACKNOWLEDGMENTS

The authors thank Dr. Harald Wodrich (Laboratoire de Microbiologie Fondamentale et Pathogénicité, Bordeaux, France) for kindly providing the U2OS-mCherry-Gal3 cells. This work was funded in part by the UMCU, the European Research Council (AdG340751), the Danish National Research Foundation (DNRF125), the Danish Cancer Society, the Swedish Research Council.

DISCLOSURE STATEMENT

No competing financial interests exist.

REFERENCES

1. Brown JM, Attardi LD: The role of apoptosis in cancer development and treatment response. *Nat Rev Cancer* 2005;5:231–237.
2. Jaattela M: Multiple cell death pathways as regulators of tumour initiation and progression. *Oncogene* 2004;23:2746–2756.
3. Yang J, Liu X, Bhalla K, *et al.*: Prevention of apoptosis by Bcl-2: release of cytochrome c from mitochondria blocked. *Science* 1997;275:1129–1132.
4. Groth-Pedersen L, Jaattela M: Combating apoptosis and multidrug resistant cancers by targeting lysosomes. *Cancer Lett* 2013;332:265–274.
5. de Duve C: Lysosomes revisited. *Eur J Biochem* 1983;137:391–397.
6. Luzio JP, Pryor PR, Bright NA: Lysosomes: fusion and function. *Nat Rev Mol Cell Biol* 2007;8:622–632.
7. Reinheckel T, Deussing J, Roth W, Peters C: Towards specific functions of lysosomal cysteine peptidases: phenotypes of mice deficient for cathepsin B or cathepsin L. *Biol Chem* 2001;382:735–741.
8. Kroemer G, Jaattela M: Lysosomes and autophagy in cell death control. *Nat Rev Cancer* 2005;5:886–897.
9. Appelqvist H, Waster P, Kagedal K, Ollinger K: The lysosome: from waste bag to potential therapeutic target. *J Mol Cell Biol* 2013;5:214–226.
10. Cesen MH, Pegan K, Spes A, Turk B: Lysosomal pathways to cell death and their therapeutic applications. *Exp Cell Res* 2012;318:1245–1251.
11. Mrschtik M, Ryan KM: Lysosomal proteins in cell death and autophagy. *FEBS J* 2015;282:1858–1870.
12. Kirkegaard T, Jaattela M: Lysosomal involvement in cell death and cancer. *Biochim Biophys Acta* 2009;1793:746–754.
13. Stoka V, Turk V, Turk B: Lysosomal cysteine cathepsins: signaling pathways in apoptosis. *Biol Chem* 2007;388:555–560.
14. Aits S, Jaattela M: Lysosomal cell death at a glance. *J Cell Sci* 2013;126:1905–1912.
15. Guicciardi ME, Leist M, Gores GJ: Lysosomes in cell death. *Oncogene* 2004;23:2881–2890.
16. De Stefanis D, Demoz M, Dragonetti A, *et al.*: Differentiation-induced changes in the content, secretion, and subcellular distribution of lysosomal cathepsins in the human colon cancer HT-29 cell line. *Cell Tissue Res* 1997;289:109–117.
17. Kallunki T, Olsen OD, Jaattela M: Cancer-associated lysosomal changes: friends or foes? *Oncogene* 2013;32:1995–2004.
18. Mohamed MM, Sloane BF: Cysteine cathepsins: multifunctional enzymes in cancer. *Nat Rev Cancer* 2006;6:764–775.
19. Fehrenbacher N, Bastholm L, Kirkegaard-Sorensen T, *et al.*: Sensitization to the lysosomal cell death pathway by oncogene-induced down-regulation of lysosome-associated membrane proteins 1 and 2. *Cancer Res* 2008;68:6623–6633.
20. Ostenfeld MS, Fehrenbacher N, Hoyer-Hansen M, Thomsen C, Farkas T, Jaattela M: Effective tumor cell death by sigma-2 receptor ligand siramesine involves lysosomal leakage and oxidative stress. *Cancer Res* 2005;65:8975–8983.
21. Feng Y, Mitchison TJ, Bender A, Young DW, Tallarico JA: Multi-parameter phenotypic profiling: using cellular effects to characterize small-molecule compounds. *Nat Rev Drug Discov* 2009;8:567–578.
22. Carpenter AE: Image-based chemical screening. *Nat Chem Biol* 2007;3:461–465.
23. Nadanaciva S, Lu S, Gebhard DF, Jessen BA, Pennie WD, Will Y: A high content screening assay for identifying lysosomotropic compounds. *Toxicol In Vitro* 2011;25:715–723.
24. Lemieux B, Percival MD, Falgueyret JP: Quantitation of the lysosomotropic character of cationic amphiphilic drugs using the fluorescent basic amine Red DND-99. *Anal Biochem* 2004;327:247–251.
25. Ostenfeld MS, Hoyer-Hansen M, Bastholm L, *et al.*: Anti-cancer agent siramesine is a lysosomotropic detergent that induces cytoprotective autophagosome accumulation. *Autophagy* 2008;4:487–499.
26. Aits S, Jaattela M, Nylandsted J: Methods for the quantification of lysosomal membrane permeabilization: a hallmark of lysosomal cell death. *Methods Cell Biol* 2015;126:261–285.
27. Paz I, Sachse M, Dupont N, *et al.*: Galectin-3, a marker for vacuole lysis by invasive pathogens. *Cell Microbiol* 2010;12:530–544.
28. Maejima I, Takahashi A, Omori H, *et al.*: Autophagy sequesters damaged lysosomes to control lysosomal biogenesis and kidney injury. *EMBO J* 2013;32:2336–2347.
29. Freeman D, Cedillos R, Choyke S, *et al.*: Alpha-synuclein induces lysosomal rupture and cathepsin dependent reactive oxygen species following endocytosis. *PLoS One* 2013;8:e62143.
30. Thurston TL, Wandel MP, von Muhlinen N, Foeglein A, Randow F: Galectin 8 targets damaged vesicles for autophagy to defend cells against bacterial invasion. *Nature* 2012;482:414–418.
31. D'Astolfo DS, Pagliero RJ, Pras A, *et al.*: Efficient intracellular delivery of native proteins. *Cell* 2015;161:674–690.
32. Aits S, Kricker J, Liu B, *et al.*: Sensitive detection of lysosomal membrane permeabilization by lysosomal galectin puncta assay. *Autophagy* 2015;11:1408–1424.
33. Perregaard J, Moltzen EK, Meier E, Sanchez C. Sigma ligands with subnanomolar affinity and preference for the sigma 2 binding site. 1. 3-(omega-aminoalkyl)-1H-indoles. *J Med Chem* 1995;38:1998–2008.
34. Sommer M, Nielsen O, Sommer M: Methods for manufacture of dihydroisobenzofuran derivatives. US patent WO 2004/026855 A1, 2004.

35. Ellegaard AM, Groth-Pedersen L, Oorschot V, *et al.*: Sunitinib and SU11652 inhibit acid sphingomyelinase, destabilize lysosomes, and inhibit multidrug resistance. *Mol Cancer Ther* 2013;12:2018–2030.
36. Maier O, Marvin SA, Wodrich H, Campbell EM, Wiethoff CM: Spatiotemporal dynamics of adenovirus membrane rupture and endosomal escape. *J Virol* 2012;86:10821–10828.
37. Zhang JH, Chung TD, Oldenburg KR: A simple statistical parameter for use in evaluation and validation of high throughput screening assays. *J Biomol Screen* 1999;4:67–73.
38. Edwards BS, Ivnitski-Steele I, Young SM, Salas VM, Sklar LA: High-throughput cytotoxicity screening by propidium iodide staining. *Curr Protoc Cytom* 2007; Chapter 9:Unit9.24.
39. Buenz EJ, Limburg PJ, Howe CL: A high-throughput 3-parameter flow cytometry-based cell death assay. *Cytometry A* 2007;71:170–173.
40. Feng J, Wang T, Zhang S, Shi W, Zhang Y: An optimized SYBR Green I/PI assay for rapid viability assessment and antibiotic susceptibility testing for Borrelia burgdorferi. *PLoS One* 2014;9:e111809.
41. Janicke RU, Sprengart ML, Wati MR, Porter AG: Caspase-3 is required for DNA fragmentation and morphological changes associated with apoptosis. *J Biol Chem* 1998;273:9357–9360.
42. Hwang J, Kim H, Kim J, *et al.*: Zinc(II) ion mediates tamoxifen-induced autophagy and cell death in MCF-7 breast cancer cell line. *Biometals* 2010;23:997–1013.
43. Kim LA, Amarnani D, Gnanaguru G, Tseng WA, Vavvas DG, D'Amore PA: Tamoxifen toxicity in cultured retinal pigment epithelial cells is mediated by concurrent regulated cell death mechanisms. *Invest Ophthalmol Vis Sci* 2014; 55:4747–4758.
44. Petersen NH, Olsen OD, Groth-Pedersen L, *et al.*: Transformation-associated changes in sphingolipid metabolism sensitize cells to lysosomal cell death induced by inhibitors of acid sphingomyelinase. *Cancer Cell* 2013;24:379–393.
45. Zong D, Zielinska-Chomej K, Juntti T, *et al.*: Harnessing the lysosome-dependent antitumor activity of phenothiazines in human small cell lung cancer. *Cell Death Dis* 2014;5:e1111.
46. Kornhuber J, Tripal P, Reichel M, *et al.*: Identification of new functional inhibitors of acid sphingomyelinase using a structure-property-activity relation model. *J Med Chem* 2008;51:219–237.
47. Antunes F, Cadenas E, Brunk UT: Apoptosis induced by exposure to a low steady-state concentration of H2O2 is a consequence of lysosomal rupture. *Biochem J* 2001;356:549–555.
48. Moriyama Y, Takano T, Ohkuma S: Acridine orange as a fluorescent probe for lysosomal proton pump. *J Biochem* 1982;92:1333–1336.
49. Varma H, Gangadhar NM, Letso RR, Wolpaw AJ, Sriramaratnam R, Stockwell BR: Identification of a small molecule that induces ATG5-and-cathepsin-l-dependent cell death and modulates polyglutamine toxicity. *Exp Cell Res* 2013;319:1759–1773.
50. Zong D, Haag P, Yakymovych I, Lewensohn R, Viktorsson K: Chemosensitization by phenothiazines in human lung cancer cells: impaired resolution of gammaH2AX and increased oxidative stress elicit apoptosis associated with lysosomal expansion and intense vacuolation. *Cell Death Dis* 2011;2:e181.
51. Sukhai MA, Prabha S, Hurren R, *et al.*: Lysosomal disruption preferentially targets acute myeloid leukemia cells and progenitors. *J Clin Invest* 2013;123:315–328.
52. Kornhuber J, Tripal P, Reichel M, *et al.*: Functional Inhibitors of Acid Sphingomyelinase (FIASMAs): a novel pharmacological group of drugs with broad clinical applications. *Cell Physiol Biochem* 2010;26:9–20.
53. Kreuger MR, Grootjans S, Biavatti MW, Vandenabeele P, D'Herde K: Sesquiterpene lactones as drugs with multiple targets in cancer treatment: focus on parthenolide. *Anticancer Drugs* 2012;23:883–896.
54. Kim SL, Liu YC, Seo SY, *et al.*: Parthenolide induces apoptosis in colitis-associated colon cancer, inhibiting NF-kappaB signaling. *Oncol Lett* 2015;9:2135–2142.
55. Wyrebska A, Gach K, Janecka A: Combined effect of parthenolide and various anti-cancer drugs or anticancer candidate substances on malignant cells in vitro and in vivo. *Mini Rev Med Chem* 2014;14:222–228.
56. Ghantous A, Gali-Muhtasib H, Vuorela H, Saliba NA, Darwiche N: What made sesquiterpene lactones reach cancer clinical trials? *Drug Discov Today* 2010;15: 668–678.
57. Tiuman TS, Ueda-Nakamura T, Garcia Cortez DA, *et al.*: Antileishmanial activity of parthenolide, a sesquiterpene lactone isolated from Tanacetum parthenium. *Antimicrob Agents Chemother* 2005;49:176–182.
58. Groth-Pedersen L, Ostenfeld MS, Hoyer-Hansen M, Nylandsted J, Jaattela M: Vincristine induces dramatic lysosomal changes and sensitizes cancer cells to lysosome-destabilizing siramesine. *Cancer Res* 2007;67:2217–2225.
59. Groth-Pedersen L, Aits S, Corcelle-Termeau E, Petersen NH, Nylandsted J, Jaattela M: Identification of cytoskeleton-associated proteins essential for lysosomal stability and survival of human cancer cells. *PLoS One* 2012;7:e45381.
60. D'Anneo A, Carlisi D, Lauricella M, *et al.*: Parthenolide generates reactive oxygen species and autophagy in MDA-MB231 cells. A soluble parthenolide analogue inhibits tumour growth and metastasis in a xenograft model of breast cancer. *Cell Death Dis* 2013;4:e891.
61. Fehrenbacher N, Jaattela M: Lysosomes as targets for cancer therapy. *Cancer Res* 2005;65:2993–2995.
62. Fehrenbacher N, Gyrd-Hansen M, Poulsen B, *et al.*: Sensitization to the lysosomal cell death pathway upon immortalization and transformation. *Cancer Res* 2004; 64:5301–5310.

Address correspondence to:
David A. Egan, PhD
Cell Biology Department
University Medical Center Utrecht (UMCU)
Heidelberglaan 100
Room H02.313
3584 CX Utrecht
Netherlands

E-mail: d.a.egan@umcutrecht.nl

Abbreviations Used

95% CI = 95% confidence interval
ASM = acid sphingomyelinase
Bcl2 = B-cell lymphoma 2 protein
CAD = cationic amphiphilic drug
Casp3 = caspase 3
DMSO = dimethyl sulfoxide
Gal-3 = galectin-3
HCS = high content screening
HT = high throughput
HTS = high-throughput screening
LAMP-1 = lysosomal-associated membrane protein 1
LC_{50} = concentration that is lethal to 50% of cells
LCD = lysosomal cell death
LMP = lysosomal membrane permeabilization
LT = lysosomotropic
mAG = monomeric Azami-green fluorescent protein
MeOH = methanol
MSAPC = Mean_SpotAreaPerCell
p53 = transformation-related protein 53
PBS = phosphate buffered saline
PCD = programmed cell death
PI = propidium iodide
SD = standard deviation
S/B = signal to background
S/N = signal to noise
wt = wild type